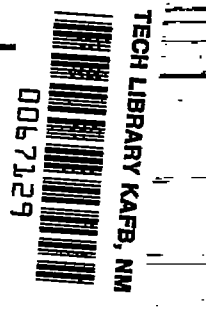


10272 0266 NT ACAN



NATIONAL ADVISORY COMMITTEE FOR AERONAUTICS

TECHNICAL NOTE 3920

EFFECT OF SPANWISE VARIATIONS IN GUST INTENSITY ON THE
LIFT DUE TO ATMOSPHERIC TURBULENCE

By Franklin W. Diederich and Joseph A. Drischler

Langley Aeronautical Laboratory
Langley Field, Va.



Washington

April 1957

AFMDC
TECHNICAL LIBRARY
AFL 2311



TECHNICAL NOTE 3920

EFFECT OF SPANWISE VARIATIONS IN GUST INTENSITY ON THE
LIFT DUE TO ATMOSPHERIC TURBULENCE

By Franklin W. Diederich and Joseph A. Drischler

SUMMARY

The method presented in NACA TN 3910 for calculating the effect of spanwise variations in gust intensity on the statistical characteristics of the response of an airplane to continuous random atmospheric turbulence is used herein to calculate the effect of these variations on the lift directly due to turbulence. Both the horizontal and the vertical components of turbulence for both swept and unswept wings are considered. Several analytic approximations to the correlation functions and power spectra of atmospheric turbulence and several spanwise weighting functions (span loadings) are used in these calculations.

The averaging effect of the span on the lift is shown to be very similar for the normal and the longitudinal components of turbulence, for the various span loadings and turbulence spectra considered herein, and for various angles of sweepback.

INTRODUCTION

The local fluctuations of air velocity experienced by an airplane flying through atmospheric turbulence constitute a random process. If the fluctuations are assumed to be stationary in a statistical sense, that is, if the statistical characteristics of the turbulence are assumed to be substantially invariant along the flight path, the techniques of generalized harmonic analysis may be used to calculate the airplane responses. (See ref. 1, for instance.)

In this approach the assumption has generally been made implicitly that the gust intensity at any one instant is substantially the same at all points on the wing. When spanwise variations in gust intensity are to be taken into account, the statistical problem becomes more difficult inasmuch as the input process is now multidimensional and the conventional techniques of generalized harmonic analysis can no longer be used directly.

This problem has been treated in references 2, 3, and 4, and the results of some calculations were presented in references 2 and 3. These

results indicate the magnitude of the effect of spanwise variations in instantaneous gust intensity on some airplane responses, including the lift. However, these results were very limited in scope inasmuch as only one atmospheric spectrum and only one spanwise weighting function were considered. Also, only spanwise variations in the normal component of atmospheric turbulence were considered.

The purpose of this paper is to present the results of calculations of the lift spectra and correlation functions for several spanwise weighting functions and various atmospheric spectra, both for the normal and the longitudinal components of turbulence. To this end, the basic relations for the lift correlation function and spectrum derived in reference 2 are restated and extended to the case of the longitudinal component of turbulence. Several analytical expressions for the spectra and weighting functions which have some of the desired characteristics are then used to perform the calculations.

The turbulence is assumed to be stationary, homogeneous, and isotropic (although the somewhat less restrictive assumption of axisymmetry would suffice for almost all the calculations presented herein, as in refs. 2 and 3). Thus, the statistical characteristics of the turbulence is assumed to be invariant under a displacement of the time or space origins, as well as under a rotation or inversion of the coordinate axes.

SYMBOLS

b	span
C	arbitrary parameter in the point (one-dimensional) correlation functions and power spectra of case 6
C_{I_α}	wing lift-curve slope
c_l	section lift coefficient
c	local chord
\bar{c}	average chord, S/b
E	complete elliptic integral of the second kind
h	dimensional unsteady-lift influence function for indicial gust penetration
h_1	dimensional unsteady-lift function for indicial gust penetration

H_1	dimensional unsteady-lift function for sinusoidal gust penetration
J_0, J_1	Bessel functions of the first kind, order 0 and 1
K	complete elliptic integral of the first kind
K_0, K_1	modified Bessel functions of the second kind, order 0 and 1
\tilde{K}_0, \tilde{K}_1	incomplete modified Bessel functions of the second kind, order 0 and 1
Ki_0	integral of K_0
k_2	dimensionless unsteady-lift function for sharp-edged gust penetration
k'	dimensionless frequency of wave number, $\omega L^*/U$
L	lift
L^*	longitudinal integral scale of turbulence
L^\dagger	lateral integral scale of turbulence
q	dynamic pressure
S	wing area
r	dimensionless lateral displacement, η/L^*
t	time
U	forward speed of airplane
u	longitudinal (horizontal) component of turbulence
v	lateral (side) component of turbulence
w	normal (vertical) component of turbulence
x	coordinate along the mean flight path
y	lateral coordinate
y^*	dimensionless lateral coordinate, $\frac{y}{b/2}$

α	angle of attack, radians
β	span ratio, b/L^*
γ	spanwise lift influence function (lift distribution for unit angle of attack in reverse flow)
Γ	autoconvolution of γ
$\hat{\Gamma}$	Fourier transform of γ
η	lateral displacement
η^*	dimensionless lateral displacement, $\frac{\eta}{b/2}$
ξ	longitudinal displacement
σ	dimensionless longitudinal displacement, ξ/L^*
Λ	angle of sweepback, deg
τ	time displacement, argument of time correlation function
ϕ	point (one-dimensional) power spectrum
$\tilde{\phi}$	single Fourier transform of two-dimensional correlation function (for isotropic turbulence, unless stated otherwise)
$\tilde{\phi}$	two-dimensional power spectrum, double Fourier transform of two-dimensional correlation function
$\hat{\phi}$	two-dimensional power spectrum, double Fourier transform of two-dimensional correlation function (for isotropic turbulence)
ϕ	dimensionless unsteady-lift function for sinusoidal gusts (Sears function)
ψ	point (one-dimensional) correlation function
$\tilde{\psi}$	two-dimensional correlation function
ω	frequency of oscillation
ω^*	dimensionless frequency, $\omega b/2U$

Subscripts:

- e effective (averaged)
 L lift
 u, v, w components of gust velocity

BASIC RELATIONS FOR THE CORRELATION FUNCTIONS
 AND SPECTRA OF THE LIFT

Normal Component of Turbulence

The material presented in this section is substantially identical to the treatment of this subject in references 2 and 3 and is given here primarily as a basis for the analysis of the longitudinal component of turbulence in the following section.

Unswept wings.- The instantaneous value of the lift due to the normal component of turbulence can be written in terms of an indicial-response influence function $h(t,y)$ as

$$L(t) = \int_{-\infty}^{\infty} \int_{-b/2}^{b/2} h(t,y) w(U(t-t_1), y) dy dt_1 \quad (1)$$

As pointed out in reference 2, if the wing is unswept, the function $h(t,y)$ can be written as the product of a function which depends only on time and a function which depends only on the distance along the span; that is,

$$h(t,y) = \frac{1}{b} h_1(t) \gamma(y) \quad (2)$$

where

$$h_1(t) = \frac{C_{L\alpha} q S}{U} \frac{d}{dt} k_2 \left(\frac{Ut}{c/2} \right)$$

$$\gamma(y) = \left(\frac{cc_l}{cC_{L\alpha}} \right)_{\alpha=1}^R$$

and k_2 is the unsteady-lift function due to gust penetration normalized with the steady-state value. The superscript R refers to reverse flow and can be disregarded for unswept wings, because the lift distribution of an unswept wing is the same in direct and reverse flow within the limitations of linearized lifting-surface theory.

Equation (1) can therefore be written as

$$L(t) = \int_{-\infty}^{\infty} h_1(t_1) dt_1 \frac{1}{b} \int_{-b/2}^{b/2} \gamma(y) w(U(t-t_1), y) dy$$

Hence, the correlation function for the lift can be written as

$$\psi_L(\tau) = \int_{-\infty}^{\infty} \int_{-\infty}^{\infty} h(t_1) h(t_2) dt_1 dt_2 \frac{1}{b^2} \int_{-b/2}^{b/2} \int_{-b/2}^{b/2} \gamma(y_1) \gamma(y_2) \tilde{\psi}_w(U(\tau+t_1-t_2), y_2-y_1) dy_1 dy_2 \quad (3)$$

where $\tilde{\psi}_w$ is a two-dimensional correlation function defined by

$$\tilde{\psi}_w(\xi, \eta) \equiv \overline{w(x, y) w(x+\xi, y+\eta)}$$

where the bar designates an average, which may be performed over time or space, in view of the assumed stationarity and homogeneity. For turbulence which is axisymmetric or isotropic, this double correlation function can be expressed in terms of the point (one-dimensional) correlation function as

$$\tilde{\psi}_w(\xi, \eta) = \psi_w(\sqrt{\xi^2 + \eta^2}) \quad (4)$$

If the effect of the spanwise variation in gust intensity is not taken into account, the double integral over the span in equation (3) is replaced by $b^2 \psi_w(U(\tau+t_1-t_2))$. Consequently, this integral represents, essentially, an "averaged" correlation function for the normal component of velocity ψ_{w_e} which may be used in the place of ψ_w in order to take into account spanwise variations in gust intensity.

With the use of equation (4) this function can be defined as

$$\psi_{w_e}(\xi) \equiv \frac{1}{b^2} \int_{-b/2}^{b/2} \int_{-b/2}^{b/2} \gamma(y_1) \gamma(y_2) \psi_w(\sqrt{\xi^2 + \eta^2}) dy_1 dy_2 \quad (5)$$

and hence

$$\psi_L(\tau) = \int_{-\infty}^{\infty} \int_{-\infty}^{\infty} h(t_1) h(t_2) \psi_{w_e}(U(\tau+t_1-t_2)) dt_1 dt_2 \quad (6)$$

The problem of obtaining ψ_L from ψ_{w_e} is identical to the one for the case where spanwise variations in gust intensity are ignored and, hence, will not be considered herein; instead, attention will be confined to the function $\psi_{w_e}(\xi)$.

The double integral of equation (5) can be reduced to a single integral by introducing the function $\Gamma(\eta)$ defined as the autoconvolution of $\gamma(y)$, namely

$$\Gamma(\eta) \equiv \frac{2}{b} \int_{-b/2}^{(b/2)-\eta} \gamma(y) \gamma(y+\eta) dy$$

In terms of this function, equation (5) can be written as

$$\psi_{w_e}(\xi) = \frac{1}{b} \int_0^b \Gamma(\eta) \psi_w(\sqrt{\xi^2 + \eta^2}) d\eta \quad (7)$$

In view of the symmetry of $\gamma(y)$, the function $\Gamma(\eta)$ can also be written as

$$\Gamma(\eta) = \frac{1}{b} \int_{-\eta/2}^{(b/2)-\eta} \gamma(y) \gamma(y+\eta) dy \quad (8)$$

and it must satisfy the property

$$\int_0^b \Gamma(\eta) d\eta = b \quad (9)$$

The power spectrum of the lift can be obtained by calculating the Fourier transform of the correlation function given by equation (3); namely,

$$\begin{aligned}\varphi_L(\omega) &= \frac{1}{\pi} \int_{-\infty}^{\infty} e^{-i\omega\tau} \psi_L(\tau) d\tau \\ &= |H_1(\omega)|^2 \varphi_{w_e}(\omega)\end{aligned}\quad (10)$$

where $H_1(\omega)$ is the Fourier transform of $h_1(t)$ and $\varphi_{w_e}(\omega)$ is an "averaged" spectrum which bears the same relation to the point spectrum as the correlation function ψ_{w_e} does to ψ_w and which is defined by

$$\begin{aligned}\varphi_{w_e}(\omega) &= \frac{1}{\pi} \int_{-\infty}^{\infty} e^{-i\omega\tau} \psi_{w_e}(U\tau) dt \\ &= \frac{1}{\pi U} \int_{-\infty}^{\infty} e^{-i\frac{\omega\xi}{U}} \psi_{w_e}(\xi) d\xi\end{aligned}\quad (11)$$

The function $H_1(\omega)$ represents the complex amplitude of the lift response to sinusoidal gusts which are uniform along the span and can be expressed as

$$H_1(\omega) = \frac{C_{L\alpha} q S}{U} \phi\left(\frac{\omega c}{2U}\right)$$

where ϕ represents the unsteady-lift function for sinusoidal gusts, sometimes referred to as the Sears function. As in the case of the correlation function, attention will be confined to φ_{w_e} because the manner of obtaining the lift spectrum from it is straightforward. (See eq. (10).)

As pointed out in references 2 and 3, an alternative method of obtaining φ_{w_e} consists in using two-dimensional spectra $\tilde{\Phi}_w(\omega, \eta)$ and $\tilde{\tilde{\Phi}}_w(\omega_1, \omega_2)$ defined for a general two-dimensional correlation function $\tilde{\psi}_w(\xi, \eta)$ as

$$\tilde{\Phi}_w(\omega, \eta) \equiv \frac{1}{\pi U} \int_{-\infty}^{\infty} e^{-i\frac{\omega\xi}{U}} \tilde{\psi}_w(\xi, \eta) d\xi\quad (12)$$

and

$$\left. \begin{aligned} \tilde{\Phi}_W(\omega_1, \omega_2) &\equiv \frac{1}{\pi^2 U^2} \int_{-\infty}^{\infty} \int_{-\infty}^{\infty} e^{-i\left(\frac{\omega_1}{U}\xi + \frac{\omega_2}{U}\eta\right)} \tilde{\Psi}_W(\xi, \eta) \, d\xi \, d\eta \\ \tilde{\Phi}_W(\omega_1, \omega_2) &= \frac{1}{\pi U} \int_{-\infty}^{\infty} e^{-\frac{i\omega_2}{U}\eta} \tilde{\Phi}_W(\omega_1, \eta) \, d\eta \end{aligned} \right\} \quad (13)$$

For axisymmetric or isotropic turbulence,

$$\tilde{\Phi}_W(\omega, \eta) = \frac{1}{\pi U} \int_{-\infty}^{\infty} e^{-\frac{i\omega}{U}\xi} \psi_W(\sqrt{\xi^2 + \eta^2}) \, d\xi$$

and $\tilde{\Phi}_W(\omega_1, \omega_2)$ becomes a function $\hat{\Phi}_W$ of only one variable,

$\omega \equiv \sqrt{\omega_1^2 + \omega_2^2}$; this function can be obtained from ψ_W directly as follows:

$$\hat{\Phi}_W(\omega) = \frac{2}{\pi U^2} \int_0^{\infty} \xi J_0\left(\frac{\omega}{U} \xi\right) \psi_W(\xi) \, d\xi$$

The spectrum $\Phi_{We}(\omega)$ can then be obtained directly from the following expressions, instead of using equation (11):

$$\Phi_{We}(\omega) = \frac{1}{b} \int_0^b \Gamma(\eta) \tilde{\Phi}_W(\omega, \eta) \, d\eta \quad (14)$$

or

$$\Phi_{We}(\omega) = \int_0^{\infty} \hat{\Gamma}^2(\omega_1) \hat{\Phi}_W(\sqrt{\omega^2 + \omega_1^2}) \, d\omega_1 \quad (15)$$

where $\Gamma(\eta)$ is the autoconvolution function defined in equation (8), and $\hat{\Gamma}(\omega)$ is the Fourier transform of $\gamma(y)$, namely

$$\hat{\Gamma}(\omega) = \frac{1}{b} \int_{-b/2}^{b/2} e^{-i\frac{\omega}{U}y} \gamma(y) dy \quad (16)$$

This function is real and symmetric because $\gamma(y)$ is symmetric.

Swept wings.- For a swept wing, equation (1) is replaced by

$$L(t) = \int_{-\infty}^{\infty} \int_{-b/2}^{b/2} h(t_1, y) w(U(t-t_1) + |y|\tan\Lambda, y) dy dt_1 \quad (17)$$

Whether the function $h(t, y)$ can still be written in the form of equation (2) is not known at present. However, in the following equation the assumption is made that equation (2) is still valid. The averaged correlation function $\psi_{we}(\xi)$ can then be written as

$$\psi_{we}(\xi) = \frac{1}{b^2} \int_{-b/2}^{b/2} \int_{-b/2}^{b/2} \gamma(y_1) \gamma(y_2) \psi_w \left(\sqrt{\left[\xi + (|y_2| - |y_1|) \tan\Lambda \right]^2 + (y_2 - y_1)^2} \right) dy_1 dy_2 \quad (18)$$

Inasmuch as y_2 and y_1 no longer appear only as the difference $(y_2 - y_1)$, equation (18) cannot be simplified to the form indicated by equation (7) and must in general be evaluated numerically.

The spectrum $\phi_{we}(\omega)$ can then be obtained by calculating (numerically) the Fourier transform of ψ_{we} . The direct expressions for ϕ_{we} given in equations (14) and (15) are not valid for the swept wing.

Longitudinal Component of Turbulence

Unswept wings.- The instantaneous value of the lift due to the longitudinal component of turbulence can be written as

$$L(t) = 2\alpha \int_{-\infty}^{\infty} \int_{-b/2}^{b/2} h(t_1, y) u(U(t-t_1), y) dy dt_1 \quad (19)$$

where the function $h(t, y)$ is the same indicial-response influence function as the one used in equation (1), provided that the angle of attack α is constant along the span.

The correlation function for this lift can be written in the form of equation (3). However, equation (4) is not valid for the longitudinal

component. Instead, for axisymmetrical turbulence the two-dimensional correlation function for the longitudinal component can be written in terms of the point (one-dimensional) correlation function for the longitudinal and lateral components as follows:

$$\tilde{\psi}_u(\xi, \eta) = \frac{\xi^2}{\xi^2 + \eta^2} \psi_u(\sqrt{\xi^2 + \eta^2}) + \frac{\eta^2}{\xi^2 + \eta^2} \psi_v(\sqrt{\xi^2 + \eta^2}) \quad (20)$$

If the function on the right side of equation (20) is substituted for $\psi_w(\sqrt{\xi^2 + \eta^2})$ in equations (5) and (7), corresponding expressions for the averaged correlation function $\psi_{ue}(\xi)$ are obtained in terms of the same functions $\gamma(y)$ and $\Gamma(\eta)$ used previously, namely

$$\psi_{ue}(\xi) = \frac{1}{b} \int_0^b \Gamma(\eta) \left[\frac{\xi^2}{\xi^2 + \eta^2} \psi_u(\sqrt{\xi^2 + \eta^2}) + \frac{\eta^2}{\xi^2 + \eta^2} \psi_v(\sqrt{\xi^2 + \eta^2}) \right] d\eta$$

Similarly, if the same substitution is effected in equation (12), an expression for $\tilde{\Phi}_u(\omega, \eta)$ is obtained; namely,

$$\tilde{\Phi}_u(\omega, \eta) \equiv \frac{1}{\pi U} \int_{-\infty}^{\infty} e^{-i\frac{\omega\xi}{U}} \left[\frac{\xi^2}{\xi^2 + \eta^2} \psi_u(\sqrt{\xi^2 + \eta^2}) + \frac{\eta^2}{\xi^2 + \eta^2} \psi_v(\sqrt{\xi^2 + \eta^2}) \right] d\xi$$

With this expression and the function $\Gamma(\eta)$ used previously, an averaged spectrum $\Phi_{ue}(\omega)$ can then be obtained from equation (11) by use of the function $\psi_{ue}(\xi)$ or, also, from equation (14) by use of $\tilde{\Phi}_u(\omega, \eta)$; thus,

$$\Phi_{ue}(\omega) = \frac{1}{b} \int_0^b \Gamma(\eta) \tilde{\Phi}_u(\omega, \eta) d\eta$$

Although a function $\tilde{\Phi}_u(\omega_1, \omega_2)$ can be calculated analogous to the function $\tilde{\Phi}_w(\omega_1, \omega_2)$, this function cannot be expressed in terms of $\sqrt{\omega_1^2 + \omega_2^2}$ alone; therefore the advantages of this approach are largely lost.

From this spectrum $\Phi_{ue}(\omega)$, the lift due to the longitudinal component of turbulence can then be obtained by use of the relation

$$\Phi_L(\omega) = 4\alpha^2 |H_1(\omega)|^2 \Phi_{u_e}(\omega) \quad (21)$$

As pointed out in reference 2, the lifts due to the normal and longitudinal components of turbulence are statistically independent for isotropic turbulence; consequently, the spectrum of the total lift due to both components is the sum of the spectra given by equations (10) and (21).

Swept wings.- The analysis of the lift on a swept wing due to the normal component of turbulence can also be modified to apply to the longitudinal component in a straightforward fashion. The function ψ_w under the integral in equation (18) must be replaced by

$$\frac{[\xi + (|y_2| - |y_1|) \tan \Lambda]^2}{R^2} \psi_u(R) + \frac{(y_2 - y_1)^2}{R^2} \psi_v(R)$$

where

$$R \equiv \sqrt{[\xi + (|y_2| - |y_1|) \tan \Lambda]^2 + (y_2 - y_1)^2}$$

and the evaluation of the resulting double integral for $\psi_{u_e}(\xi)$ must again be effected by numerical methods, as must the calculation of $\Phi_{u_e}(\omega)$ from this function $\psi_{u_e}(\xi)$.

If, in the preceding section (dealing with the normal component of turbulence for swept and unswept wings) the turbulence is assumed to be only axisymmetric and not isotropic, the functions $\psi_v(\xi)$ and $\psi_w(\xi)$ are not identical; the relation between them depends on the variation of the statistical characteristics of the turbulence in a direction perpendicular to the xy-plane. However, if complete isotropy is assumed, ψ_v and ψ_w are identical, and a definite relation exists between ψ_v , ψ_w , and ψ_u which will be given in the following section; equation (10) can then be expressed in terms of ψ_u alone or ψ_w alone. However, little practical advantage is gained in this manner.

WEIGHTING FUNCTIONS AND SPECTRA USED IN THE CALCULATIONS

Weighting Functions

The lift influence function $\gamma(y)$, which has been identified with the lift distribution due to unit angle of attack in reverse flow, serves

as a weighting function in the integral expression for ψ_{we} , ψ_{ue} , ϕ_{we} , and ϕ_{ue} in terms of the point correlation functions and spectra. The functions used herein for the purpose of indicating the effect of changes in $\gamma(y)$ on the averaged correlation functions and spectra are given by the simple analytic expressions listed in table 1 and are shown in figure 1; they will be referred to as rectangular, elliptic, triangular, and parabolic distribution, respectively. All functions satisfy the condition

$$\int_{-b/2}^{b/2} \gamma(y) dy = b$$

which follows from the definition of $\gamma(y)$. The function designated as rectangular distribution is the one that has been used in references 2 and 3. The corresponding functions $\Gamma(\eta)$ and $\hat{\Gamma}(\omega)$ are also given in table 1, and the function $\Gamma(\eta)$ is shown in figure 1.

For functions other than those considered herein (which can be obtained for any given wing from reference 5 or a similar compilation of spanwise lift distributions), the functions $\Gamma(\eta)$ and $\hat{\Gamma}(\omega)$ must be calculated numerically. The integrating factors I_{1j} given in table 2 have been found useful for calculating $\Gamma(\eta)$. These factors apply to the case where values of $\gamma(y)$ are used at every tenth of the semispan and where $\Gamma(\eta)$ is obtained at every tenth of the span by use of the relation

$$\Gamma(\eta_i) = \frac{1}{b} \sum_{j=-1}^{9-2i} I_{1j} \gamma(y_j) \gamma(y_j + \eta_i)$$

with

$$\eta_i = \frac{i}{10} b \quad y_j = \frac{j}{10} \frac{b}{2}$$

where $i = 0, 1, \dots, 9$ and $j = -9, -8, \dots, 8, 9$. The value of $\Gamma(b)$ is always zero; therefore no factors are listed for $i = 10$. These factors apply to functions $\gamma(y)$ which go to zero at the wing tips as the square root of the distance from the tips, as spanwise lift distributions in subsonic and supersonic flow usually do.

Point Correlation Functions and Spectra

General relations.- In isotropic turbulence the mean-square values of the u , v , and w components of the turbulence are identical; that

is, $\overline{u^2} = \overline{v^2} = \overline{w^2}$. The point correlation functions for these components (for flight parallel to the u component) can be expressed in terms of each other by means of the relation given in reference 6; namely,

$$\psi_v(\xi) = \psi_w(\xi)$$

$$\psi_w(\xi) = \psi_u(\xi) + \frac{\xi}{2} \frac{d}{d\xi} \psi_u(\xi) \quad (22)$$

This ordinary differential equation for $\psi_u(\xi)$ with the boundary condition $\psi_u(0) \neq \psi_w(0)$ can be solved to yield the following expression:

$$\psi_u(\xi) = \frac{2}{\xi^2} \int_0^\xi \xi_1 \psi_w(\xi_1) d\xi_1 \quad (23)$$

Hence, the power spectra corresponding to these correlation functions must satisfy the relation

$$\phi_w(\omega) = \frac{1}{2} \left[\phi_u(\omega) - \omega \frac{d}{d\omega} \phi_u(\omega) \right] \quad (24)$$

Moreover, the solution of this equation for $\phi_u(\omega)$ with the boundary condition $\phi_u(\infty) = 0$ yields

$$\phi_u(\omega) = 2\omega \int_\omega^\infty \frac{\phi_w(\omega_1)}{\omega_1^2} d\omega_1 \quad (25)$$

The integral scales of turbulence L^* and L^\dagger are defined as

$$\begin{aligned} L^* &\equiv \frac{1}{u^2} \int_0^\infty \psi_u(\xi) d\xi \\ &= \frac{\pi}{2} \frac{U}{u^2} \phi_u(0) \end{aligned}$$

and

$$\begin{aligned} L^{\dagger} &\equiv \frac{1}{w^2} \int_0^{\infty} \psi_w(\xi) d\xi \\ &= \frac{\pi}{2} \frac{U}{w^2} \phi_w(0) \end{aligned}$$

As a result of equation (22)

$$L^{\dagger} = \frac{1}{2} L^*$$

for isotropic turbulence, as can be shown by integrating the second term on the right side of equation (22) by parts. Also, as a result of equation (22), the moment of the lateral correlation function can be shown to be zero; that is,

$$\int_0^{\infty} \psi_w(\xi) \xi d\xi = 0$$

provided that $\psi_w(\xi)$ goes to zero more rapidly than $1/\xi^2$ when ξ becomes very large - a condition which any actual correlation function must satisfy. This condition on the moment of $\psi_w(\xi)$ implies that for isotropic turbulence any actual lateral correlation function must be negative for some values of ξ .

Specific expressions used in calculations.- The point correlation functions and spectra used in the calculations are listed in table 3. The one labeled "case 1" is the one used previously in references 2 and 3. Although the spectra do not have finite moments (so that the mean-square values of the derivatives of u , v , and w are infinite), they appear to fit available experimental data on turbulence in the atmosphere and in wind tunnels fairly well, except at very high and very low frequencies. At very low frequencies some of the responses of airplanes are very small; thus, despite their theoretical shortcomings, these spectra are often very useful.

The functions of case 2 are based on an exponential approximation to the lateral correlation function and suffer not only from the shortcomings of the functions of case 1 but also violate the condition of zero moment for the function $\psi_w(\xi)$. However, case 2 represents some results of turbulence measurements in wind tunnels fairly well. (See ref. 7, for instance.)

The functions designated by case 3 and case 4 represent fittings of $\psi_u(\xi)$ and $\psi_w(\xi)$, respectively, by functions of the form $e^{-K\xi^2}$, so that the spectra contain the factor $e^{-K'\omega^2}$. Although the functions of case 4 violate the condition of zero moment for $\psi_w(\xi)$, both cases may be used to represent all or part of some wind-tunnel measurements of turbulence. (See ref. 8.) Furthermore, turbulence theory (ref. 9, for instance) indicates that a certain frequency range of the turbulence spectrum should contain a factor $e^{-K'\omega^2}$.

The spectrum $\phi_u(\omega)$ of case 5 represents, essentially, an interpolation formula suggested in reference 10, where for a certain frequency range, the three-dimensional (Heisenberg) spectrum of isotropic turbulence is assumed to be proportional to $\omega^4 \left[1 + \left(\frac{\omega}{\omega_0} \right)^2 \right]^{-17/6}$ so that the corresponding one-dimensional spectrum $\phi_u(\omega)$ used herein would be proportional to $\left[1 + \left(\frac{\omega}{\omega_0} \right)^2 \right]^{-5/6}$. The constant of proportionality can be determined from the fact that $\psi_u(0) = \overline{u^2}$, and the constant ω_0 can be related to the scale of turbulence. The resulting expression for $\psi_u(\xi)$ is the one given in table 3; the other expressions then follow from equation (22) and the definitions of the spectra. The constant 0.59253 represents $\sqrt[3]{4}/\Gamma(\frac{1}{3})$, and the constant 1.339 represents $\sqrt{\pi}\Gamma(\frac{1}{3})/\Gamma(\frac{5}{6})$, where Γ represents the gamma function. These correlation functions violate the conditions on the derivatives of a correlation function or the moments of its spectrum, just as the ones of case 1 do; but for a certain range of distances or frequencies, they may serve as useful approximations in some instances.

Case 6 represents case 1 with a correction which makes the second moment of the spectra finite; consequently, the mean-square values of the first derivatives exist, although the higher moments and, hence, the mean-square values of the higher derivatives do not exist. The constant C is arbitrary and can be used to select a frequency at which the point spectra start deviating from a second-power variation with frequency and decreasing more rapidly. On the basis of the measurements reported in reference 1, a value of $C = 50$ appears appropriate and was used in the calculations of the present paper. The expressions given in table 3 for case 6 are not entirely consistent with those for the other cases. In order to be consistent, σ should be multiplied by $(1 + C^{-2})$, k' should be divided by this quantity, and the expressions given for $\phi_u(\omega)$ and $\phi_w(\omega)$ should be divided by this quantity. However, by virtue

of the fact that this quantity differs from unity by only 0.04 percent for $C = 50$, this refinement has been ignored in order to simplify the expressions; it might have been worthwhile if a smaller value of C had been selected.

The normal point correlation functions considered herein are shown in figure 2, the longitudinal point correlation functions in figure 3, the normal point spectra in figure 4, and the longitudinal spectra in figure 5. In all these figures, the point correlation functions and spectra are given by the curves for $\beta = 0$ when not specifically referred to as point correlation functions and spectra. The correlation functions for case 6 with $C = 50$ are virtually indistinguishable from those for case 1, except for very small values of ξ ; that is, ξ/L^* less than 0.1. Similarly, the spectra are indistinguishable except for very high frequencies ($\omega L^*/U$ greater than 50), for which the spectra of case 1 attenuate as ω^{-2} , whereas those of case 6 attenuate as ω^{-4} .

Which of these cases best represents the actual characteristics of atmospheric turbulence is not known at present. Each case (except possibly cases 2 and 4) has some features which atmospheric turbulence is likely to possess, but each also has certain shortcomings. Case 1, by virtue of its simplicity and the fact that measured atmospheric spectra have large ranges in which they appear to attenuate as ω^{-2} , is probably the best choice for calculations where the behavior of the spectra at very high frequencies is not very important; when it is important, the correction represented by case 6 is likely to be sufficient for many purposes to take the more rapid rate of decrease of the spectra at high frequencies into account.

RESULTS AND DISCUSSION

Two-Dimensional Spectra

The two-dimensional spectra $\tilde{\Phi}_u(\omega, \eta)$, $\tilde{\Phi}_w(\omega, \eta)$, and $\hat{\Phi}_w(\omega)$ are given in table 4 for five of the six point correlation functions and spectra given in table 3. Again, for case 6 the values of k' and of the spectra $\tilde{\Phi}_u(\omega, \eta)$ and $\tilde{\Phi}_w(\omega, \eta)$ should be divided by $1 + C^{-2}$, and the value of $\hat{\Phi}_w(\omega)$ should be divided by the square of this quantity if this refinement is considered worthwhile.

Mean-Square Value of the Averaged Normal and Longitudinal
Component of Turbulence

The mean-square values of the averaged normal and longitudinal component of turbulence defined by

$$\overline{w_e^2} \equiv \psi_{w_e}(0)$$

and

$$\overline{u_e^2} \equiv \psi_{u_e}(0)$$

have no direct physical significance. If the wing responds equally to sinusoidal gusts of all frequencies, so that $\phi(\omega) = 1$, the mean-square lift is proportional to these quantities, although for actual unsteady-lift functions $\phi(\omega)$ they have no direct relation to the lift. Nonetheless, they serve as convenient quantities to normalize the effective or averaged correlation functions and will be used for that purpose. The power spectra can also be normalized with them, but the point mean-square value serves equally well for this purpose.

For isotropic turbulence the two quantities $\overline{w_e^2}$ and $\overline{u_e^2}$ can readily be shown to be identical for unswept wings; therefore a distinction is made between these quantities in this section for swept wings only.

The values of $\overline{w_e^2}$ calculated for the various point spectra are shown in figure 6(a) for unswept wings and rectangular loading as a function of the span ratio b/L^* . The analytical expressions for these curves are given in table 5. The manner in which $\overline{w_e^2}$ decreases with increasing span may be seen to depend to a large extent on the nature of the point correlation functions for small span ratios (where $\overline{w_e^2}$ differs relatively little from $\overline{w^2}$). For very large spans (that is, as $\beta \rightarrow \infty$), the following asymptotic relation can be shown to exist:

$$\overline{w_e^2} \sim \frac{\Gamma(0)}{2\beta} \quad (26)$$

Therefore the curves shown in figure 6(b), with the exception of the one labeled "elliptic loading," would tend to coalesce for very large span

ratios. This region of span ratios is not of direct interest for airplanes, but may be of interest for tests of the response of airplane models to wind-tunnel turbulence.

For a swept wing, $\overline{u_e^2}$ and $\overline{w_e^2}$ are not identical. They have been calculated (fig. 6(a)) for rectangular loading and the point correlation function of case 1 for a span ratio $b/L^* \cos \Lambda = 0.5$ as a function of Λ . (The angle Λ is there designated as the angle of sweepback, but could be the angle of sweepforward as well.) They may be seen to differ relatively little from each other or from their value at zero sweepback.

The effect of the shape of the loading function $\gamma(y)$ on $\overline{w_e^2}$ may be seen in figure 6(d), where $\overline{w_e^2}/w^2$ is shown as a function of b/L^* for unswept wings, for the point correlation function of case 1, and for four different loading functions. For small span ratios the effect of changes in γ is fairly small; only for very large span ratios does the effect become significant, as may also be seen from equation (26). Similar calculations have also been made numerically for the point correlation function of case 5 for rectangular and elliptic loadings; the results are shown in figure 6(b) and corroborate the conclusion reached from the results obtained with the point correlation functions of case 1.

Correlation Functions of the Averaged Components of Turbulence

The functions ψ_{w_e} and ψ_{u_e} calculated for the point correlations of cases 1 to 5 for unswept wings with rectangular loadings are shown in figures 2 and 3, where they have been normalized with $\overline{w_e^2}$. The corresponding analytical expressions are given in tables 5 and 6. Inasmuch as no tables of incomplete modified Bessel functions were available, the functions for cases 1 and 5 were calculated numerically and those for case 2 were obtained from reference 7 where they were also calculated numerically.

The effect of the span ratio b/L^* on the normalized correlation functions may be seen to be fairly small and in some cases nil, namely ψ_{u_e} for case 3 and ψ_{w_e} for case 4. This effect appears to be substantially the same on both ψ_{u_e} and ψ_{w_e} , as may be seen by comparing figures 2(a) and 3(b). The nature of the effect depends on the point correlation functions. For instance, in the range of ξ/L^* from 0 to 2, the normalized functions ψ_{w_e} tend to increase with β for cases 1, 2, 5, and 6, but to decrease or be unchanged for cases 3 and 4. The functions labeled $\beta \rightarrow \infty$ pertain to span ratios so large that $\overline{w_e^2}$ is given

by equation (26) with sufficient accuracy and are, again, not directly pertinent to actual airplanes but are shown primarily as a theoretical limiting case.

The effective correlation functions ψ_{w_e} and ψ_{u_e} for swept wings with $b/L \cos \Lambda = 0.5$ and rectangular loading and for the point correlation functions of case 1 are shown in figures 7(a) and 7(b). When these functions are normalized with w_e^2 and u_e^2 , respectively, they are not affected by sweep to an appreciable extent. These effective correlative functions were calculated from the integral expressions given in this paper by use of a combination of numerical and graphical techniques.

Some calculations of the effective correlation functions were also made for elliptic span loading or weighting functions $\gamma(y)$, by use of numerical methods and are shown in figures 2(a), 2(d), and 3(b). The differences between them and those for rectangular loading may be seen to be very small if the functions are normalized with w_e^2 .

Spectra of the Averaged Components of Turbulence

The functions ϕ_{w_e} and ϕ_{u_e} calculated for the various point correlation functions for unswept wings with rectangular loadings are shown in figures 4 and 5. In figures 4(b), 4(g), and 5(c), these functions have been normalized with w^2 , but in the other parts of these figures they have been normalized with w_e^2 and thus represent directly the Fourier transforms of the functions ψ_{w_e} and ψ_{u_e} normalized with w_e^2 . The analytic expressions for these functions are given in tables 5 and 6.

An examination of these figures indicates that, regardless of whether the spectra are normalized with w_e^2 or w^2 , the effect of spanwise variations in gust intensity on the spectra appears to be larger than the effect on the correlation functions. From figures 4(b) and 5(a) may be seen the fact that this averaging process tends to reduce the magnitude of the spectra at all frequencies, but to the largest extent at high frequencies, as may be expected. For the point spectra of cases 1, 5, and 6, which attenuate at high frequencies as ω^{-2} , $\omega^{-5/3}$, and ω^{-4} respectively, the effective spectra attenuate as ω^{-3} , $\omega^{-8/3}$, and ω^{-5} , respectively. This fact may be seen from figures 4 and 5 and follows from the asymptotic relation for $\omega \rightarrow \infty$:

$$\phi_{w_e}(\omega) \sim \frac{1}{2} \frac{U\Gamma(0)}{b} \hat{\phi}_w(\omega) \quad (27)$$

and from a similar relation for ϕ_{u_e} ; for instance, for case 1 and rectangular loading

$$\frac{\phi_{w_e}(\omega)}{\overline{w^2 L^*} / U} \sim \frac{3}{\beta k'^3}$$

whereas

$$\frac{\phi_w(\omega)}{\overline{w^2 L^*} / U} \sim \frac{3}{\pi k'^2}$$

Again, the nature of the effect of averaging is substantially the same for ϕ_{u_e} and ϕ_{w_e} , but appears to depend to some extent on the point correlation function, the effect being fairly large for the point correlation functions of cases 1, 2, 5, and 6 and relatively small or nil for those of cases 3 and 4.

The effect of sweep on the effective normal and longitudinal spectra may be seen from figures 7(c) and 7(d) to be very small for the given value $b/L^* \cos \Lambda = 0.5$, provided that the spectra are normalized with $\overline{w_e^2}$ and $\overline{u_e^2}$, respectively. These spectra were calculated by performing the Fourier transforms of ψ_{w_e} and ψ_{u_e} for these cases numerically, and the results of these calculations are somewhat uncertain at high frequencies. Therefore these functions are shown only for frequencies up to $\omega L^*/U = 20$ and may be valid only for $\omega L^*/U$ below about 10. The possibility exists, therefore, that the spectra for swept wings differ from those for unswept wings at very high frequencies, even when normalized with $\overline{w_e^2}$.

The effect of changes in the shape of $\gamma(y)$ on the effective spectra may be seen from figure 4(g), where the spectra are shown for unswept wings with $b/L^* = 0.5$ and for the point correlation functions of case 1, but for several loadings. These spectra were normalized with $\overline{w^2}$ in order to emphasize the effects of the shape of the loading. Even so, these effects are small, except at very high frequencies, as may also be seen from equation (27). If the functions had been normalized with $\overline{w_e^2}$, these effects would have been even less pronounced. For some other point correlation functions, calculations have been made numerically for elliptic as well as rectangular loadings. The results, normalized with $\overline{w_e^2}$, are shown in figures 4(a), 4(e), and 5(b) and may be seen to differ very little from the corresponding ones for rectangular loading.

Effective Scales of Turbulence

Effective or apparent scales of turbulence can be defined in a manner analogous to that for the actual scales of turbulence, namely

$$\begin{aligned} L_e^* &\equiv \frac{1}{u_e^2} \int_0^\infty \psi_{u_e}(\xi) d\xi \\ &= \frac{\pi}{2} \frac{U}{u_e^2} \phi_{u_e}(0) \end{aligned}$$

and

$$\begin{aligned} L_e^\dagger &= \frac{1}{w_e^2} \int_0^\infty \psi_{w_e}(\xi) d\xi \\ &= \frac{\pi}{2} \frac{U}{w_e^2} \phi_{w_e}(0) \end{aligned}$$

These parameters may therefore be deduced from the relations for the spectra given in tables 5 and 6 for $\omega = 0$ and are shown in figure 8 as functions of the span ratio b/L^* for the various point correlation functions used herein. Figures 8(b) and 8(d) pertain to unswept wings, and figures 8(a) and 8(c) pertain to swept wings with $b/L^* \cos \Lambda = 0.5$ and rectangular loading.

The averaging effect of the span on these scales depends on the point correlation functions and appears to be fairly small for small span ratios; it is similar for both L_e^* and L_e^\dagger . For instance, L_e^\dagger tends to increase as the span increases for the point correlation functions of cases 1, 2, 5, and 6 and to decrease for case 3; it is independent of the span for case 4.

As may be seen from figures 8(a) and 8(c) the effect of sweep on L_e^\dagger and L_e^* appears to be very small for given values of $b/L^* \cos \Lambda$. Similarly, the effect of changes in the shape of $\gamma(y)$ on L_e^\dagger and L_e^* may be seen to be fairly small from figures 8(b) and 8(d), where for some point correlation functions results are shown not only for rectangular loadings but also for elliptic, parabolic, and triangular loadings.

In figures 8(b) and 8(d) the rays for constant b/L_e^\dagger and b/L_e^* have been drawn in. The purpose of this addition to the figures was to facilitate the problem of determining a value of L^* or L^\dagger from lift measurements on a wing of finite span. In this problem Φ_{w_e} and Φ_{u_e} can be deduced if the unsteady-lift function and the lift spectrum are known. Hence, L_e^* or L_e^\dagger is known, as is the span of the wing; therefore, the ratio b/L_e^* or b/L_e^\dagger is known. The intersection of the ray for that ratio with the curve for the case for which the shapes of the averaged spectra most nearly resemble that of the spectrum obtained from the measurements establishes the values of L_e^\dagger/L^\dagger or L_e^*/L^* and of b/L^* , from any of which the value of L^* can be determined directly.

CONCLUSIONS

The correlation functions and spectra for a suitably weighted instantaneous average of the intensity of the normal and longitudinal components of atmospheric turbulence have been calculated for isotropic turbulence by the method of NACA TN 3910. Several analytic expressions were used for the point correlation functions or spectra and for the lift influence function (weighting function). These averaged correlation functions and spectra bear the same relation to those for the lift as do the point correlation functions and spectra, except that they take into account the instantaneous variations in gust intensity over the span; whereas the use of the point correlation functions and spectra implies that the gust intensity is assumed to be constant along the span at any instant. Consequently, the following conclusions concerning the averaged or effective gust intensity pertain directly to the power spectrum of the lift:

1. The effect of spanwise variations in gust intensity is to decrease, essentially, the mean-square gust intensity experienced by the wing. The extent of this decrease is small when the span is small, but increases as the span increases; the rate at which it increases depends on the shapes of the point correlation functions and of the weighting functions. The effective mean-square longitudinal and normal components are the same for unswept wings (in isotropic turbulence) but differ slightly for swept wings.

2. Apart from this overall decrease in level, the correlation functions are relatively insensitive to changes in span, provided that the span is small compared with the scale of turbulence as is the case for actual airplanes. The small changes in the shape of the correlation functions depend primarily on the shape of the point correlation function

and, to a lesser extent, on the shape of the weighting functions and the angle of sweepback, and are similar for the normal and longitudinal component of turbulence.

3. The instantaneous spanwise variations in gust intensity result in a decrease of the spectra at all frequencies, but most significantly at the highest frequencies. The extent of this decrease becomes greater as the span increases and depends on the shape of the point power spectra, but is less sensitive to variations in the spanwise weighting function and to the angle of sweepback, except at very high frequencies; also this decrease is similar for the normal and longitudinal component of turbulence.

4. The scales of turbulence are affected relatively little by changes in span, at least for spans which are small compared with the scale of turbulence. The slight changes in the scales depend primarily on the point correlation functions or spectra and may represent either an increase or a decrease of the apparent scales; they are not affected appreciably by the shape of the spanwise loading function and the angle of sweepback.

Langley Aeronautical Laboratory,
National Advisory Committee for Aeronautics,
Langley Field, Va., November 2, 1956.

REFERENCES

1. Press, Harry, and Houbolt, John C.: Some Applications of Generalized Harmonic Analysis to Gust Loads on Airplanes. Jour. Aero. Sci., vol. 22, no. 1, Jan. 1955, pp. 17-26, 60.
2. Diederich, Franklin W.: The Response of an Airplane to Random Atmospheric Disturbances. NACA TN 3910, 1957.
3. Diederich, Franklin W.: The Dynamic Response of a Large Airplane to Continuous Random Atmospheric Disturbances. Jour. Aero. Sci., vol. 23, no. 10, Oct. 1956, pp. 917-930.
4. Liepmann, H. W.: Extension of the Statistical Approach to Buffeting and Gust Response of Wings of Finite Span. Jour. Aero. Sci., vol. 22, no. 3, Mar. 1955, pp. 197-200.
5. Diederich, Franklin W., and Zlotnick, Martin: Calculated Spanwise Lift Distributions, Influence Functions, and Influence Coefficients for Unswept Wings in Subsonic Flow. NACA Rep. 1228, 1955. (Supersedes NACA TN 3014.)
6. Von Kármán, Theodor, and Howarth, Leslie: On the Statistical Theory of Isotropic Turbulence. Proc. Roy. Soc. (London), ser. A, vol. 164, no. 917, Jan. 21, 1938, pp. 192-215.
7. Dryden, Hugh L., Schubauer, G. B., Mock, W. C., Jr., and Skramstad, H. K.: Measurements of Intensity and Scale of Wind-Tunnel Turbulence and Their Relation to the Critical Reynolds Number of Spheres. NACA Rep. 581, 1937.
8. Frenkiel, Francois N.: Étude Statistique de la Turbulence - Fonctions Spectrales et Coefficients de Corrélation (Statistical Study of Turbulence - Spectral Functions and Correlation Coefficients). O.N.E.R.A. Rapport Tech. No. 34, 1948.
9. Von Kármán, Th., and Lin, C. C.: On the Statistical Theory of Isotropic Turbulence. Vol. II of Advances in Applied Mechanics, Richard von Mises and Theodore von Kármán, eds., Academic Press, Inc. (New York), 1951, pp. 1-19.
10. Von Kármán, Theodore: Progress in the Statistical Theory of Turbulence. Proc. Nat. Acad. Sci., vol. 34, no. 11, Nov. 1948, pp. 530-539.

TABLE 1.- WEIGHTING FUNCTIONS $\gamma(y)$ AND CORRESPONDING FUNCTIONS $\Gamma(\eta)$ AND $\hat{\Gamma}(\omega)$

Shape of weighting function	$\gamma(y)$	$\Gamma(\eta)$	$\hat{\Gamma}(\omega)$
Rectangular	1	$2 - \eta^*$	$\frac{\sin \omega^*}{\omega^*}$
Elliptic	$\frac{4}{\pi} \sqrt{1 - y^{*2}}$	$\frac{32}{3\pi^2} (2 + \eta^*) \left[\left(1 + \frac{1}{4} \eta^{*2}\right) E\left(\frac{2-\eta^*}{2+\eta^*}\right) - \eta^* K\left(\frac{2-\eta^*}{2+\eta^*}\right) \right]$	$2 \frac{J_1(\omega^*)}{\omega^*}$
Triangular	$2(1 - y^*)$	$\begin{cases} \frac{2}{3}(4 - 6\eta^{*2} + 3\eta^{*3}) & 0 \leq \eta \leq \frac{b}{2} \\ \frac{2}{3}(8 - 12\eta^* + 6\eta^{*2} - \eta^{*3}) & \frac{b}{2} \leq \eta \leq b \end{cases}$	$2 \frac{1 - \cos \omega^*}{\omega^{*2}}$
Parabolic	$\frac{3}{2}(1 - y^{*2})$	$\frac{3}{40}(32 - 40\eta^{*2} + 20\eta^{*3} - \eta^{*5})$	$3 \frac{\sin \omega^* - \omega^* \cos \omega^*}{\omega^{*3}}$

TABLE 2.- THE INTEGRATING FACTOR I_{1j} FOR NUMERICAL EVALUATION OF $\Gamma(\eta_i)$ FROM $\gamma(y_j)$

j	i = 0	i = 1	i = 2	i = 3	i = 4	i = 5	i = 6	i = 7	i = 8	i = 9
-9										0.15708
-8									0.09562	
-7								0.13333	.25333	
-6							0.13333	.12000		
-5						0.13333	.13333	.30170		
-4					0.13333	.13333	.22896			
-3				0.13333	.13333	.26667	.25333			
-2			0.13333	.13333	.26667	.12000				
-1		0.13333	.13333	.26667	.13333	.30170				
0	0.13333	.13333	.26667	.13333	.22896					
1	.13333	.26667	.13333	.26667	.25333					
2	.26667	.13333	.26667	.12000						
3	.13333	.26667	.13333	.30170						
4	.26667	.13333	.22896							
5	.13333	.26667	.25333							
6	.26667	.12000								
7	.13333	.30170								
8	.25000									
9	.20000									

TABLE 3.- POINT CORRELATION FUNCTIONS AND SPECTRA

Case	$\frac{\psi_u(t)}{u^2}$	$\frac{\psi_v(t)}{v^2}$	$\frac{\phi_u(\omega)}{u^2 L^* / U}$	$\frac{\phi_v(\omega)}{v^2 L^* / U}$
1	$e^{- \sigma }$	$\left(1 - \frac{ \sigma }{2}\right) e^{- \sigma }$	$\frac{2}{\pi} \frac{1}{1 + k'^2}$	$\frac{1}{\pi} \frac{1 + 3k'^2}{(1 + k'^2)^2}$
2	$\frac{1 - e^{-2 \sigma } - 2 \sigma e^{-2 \sigma }}{(2\sigma)^2}$	$e^{-2 \sigma }$	$\frac{2}{\pi} \left(1 - \frac{k'}{2} \tan^{-1} \frac{2}{k'}\right)$	$\frac{1}{\pi} \frac{1}{1 + (k'/2)^2}$
3	$\frac{\pi \sigma^2}{k}$	$\left(1 - \frac{\pi}{4} \sigma^2\right) e^{-\frac{\pi \sigma^2}{4}}$	$\frac{2}{\pi} e^{-\frac{k'^2}{\pi}}$	$\frac{1}{\pi} e^{-\frac{k'^2}{\pi}} \left(1 + 2 \frac{k'^2}{\pi}\right)$
4	$\frac{1 - e^{-\pi \sigma^2}}{\pi \sigma^2}$	$e^{-\pi \sigma^2}$	$\frac{2}{\pi} \left[e^{-\frac{k'^2}{4\pi}} - \frac{k'}{2} \left(1 - \operatorname{erf} \frac{k'}{2\sqrt{\pi}}\right) \right]$	$\frac{1}{\pi} e^{-\frac{k'^2}{4\pi}}$
5	$0.59253 \sqrt{\frac{\sigma}{1.339}} K_{1/3} \left(\frac{\sigma}{1.339}\right)$	$0.59253 \sqrt{\frac{\sigma}{1.339}} \left[K_{1/3} \left(\frac{\sigma}{1.339}\right) - \frac{1}{2} \frac{\sigma}{1.339} K_{2/3} \left(\frac{\sigma}{1.339}\right) \right]$	$\frac{2}{\pi} \frac{1}{[1 + (1.339k')^2]^{5/6}}$	$\frac{1}{\pi} \frac{1 + \frac{8}{5}(1.339k')^2}{[1 + (1.339k')^2]^{11/6}}$
6	$e^{- \sigma } + \sigma e^{-c \sigma }$	$\left(1 - \frac{ \sigma }{2}\right) e^{- \sigma } + \left(\frac{3}{2} \sigma - \frac{c}{2}\sigma^2\right) e^{-c \sigma }$	$\frac{2}{\pi} \left[\frac{1}{1 + k'^2} + \frac{c^2 - k'^2}{(c^2 + k'^2)^2} \right]$	$\frac{1}{\pi} \left[\frac{1 + 3k'^2}{(1 + k'^2)^2} + \frac{c^4 + 6c^2 k'^2 - 3k'^4}{(c^2 + k'^2)^3} \right]$

TABLE 4.- TWO-DIMENSIONAL SPECTRA

Case	$\frac{\tilde{\Phi}_w(\omega, \eta)}{v^2 L^* / U}$	$\frac{\tilde{\Phi}_u(\omega, \eta)}{v^2 L^* / U}$	$\frac{\hat{\Phi}_w(\omega)}{v^2 L^{*2} / U^2}$
1	$\frac{1}{\pi} \left[\frac{1 + 3k'^2}{(1 + k'^2)^{3/2}} r K_1(x\sqrt{1+k'^2}) - \frac{r^2}{1 + k'^2} K_0(x\sqrt{1+k'^2}) \right]$	$\frac{2}{\pi} \left[\frac{r}{\sqrt{1 + k'^2}} K_1(x\sqrt{1+k'^2}) - \frac{k'^2}{2} K_0(x\sqrt{1+k'^2}) \right]$	$\frac{3}{\pi} \frac{k'^2}{(1 + k'^2)^{5/2}}$
2	$\frac{4}{\pi} \frac{r}{\sqrt{4 + k'^2}} K_1(x\sqrt{4+k'^2})$		$\frac{4}{\pi} \frac{1}{(4 + k'^2)^{3/2}}$
3	$\frac{1}{\pi} \left(1 - \frac{\pi}{2} r^2 + \frac{2}{\pi} k'^2 \right) e^{-\frac{k'^2}{\pi}} e^{-\frac{\pi}{4} r^2}$	$\frac{2}{\pi} \left(1 - \frac{\pi}{4} r^2 \right) e^{-\frac{k'^2}{\pi}} e^{-\frac{\pi}{4} r^2}$	$\frac{4}{\pi^3} k'^2 e^{-\frac{k'^2}{\pi}}$
4	$\frac{1}{\pi} e^{-\frac{\pi r^2 - k'^2}{4\pi}}$		$\frac{1}{\pi^2} e^{-\frac{k'^2}{4\pi}}$
6	<p>Same as case 1, plus:</p> $\frac{1}{\pi} \left[\frac{2c^2(c^2 + 3k'^2)r^2}{(c^2 + k'^2)^2} K_0(x\sqrt{c^2 + k'^2}) + \frac{(c^4 + 6c^2k'^2 - 3k'^4)r - c^4(c^2 + k'^2)r^3}{(c^2 + k'^2)^{5/2}} K_1(x\sqrt{c^2 + k'^2}) \right]$	<p>Same as case 1, plus:</p> $\frac{1}{\pi} \left[\left(\frac{3c^2 + k'^2}{c^2 + k'^2} \right) r^2 K_0(x\sqrt{c^2 + k'^2}) + \frac{2(c^2 - k'^2)r - c^2(c^2 + k'^2)r^3}{(c^2 + k'^2)^{3/2}} K_1(x\sqrt{c^2 + k'^2}) \right]$	<p>Same as case 1, plus:</p> $\frac{3}{\pi} \frac{4c^2k'^2 - k'^4}{(c^2 + k'^2)^{7/2}}$

TABLE 5.- AVERAGED CORRELATION FUNCTIONS AND POWER SPECTRA FOR VERTICAL COMPONENT OF TURBULENCE

[Rectangular loading; unswept wings]

Case	$\frac{\overline{v_c^2}}{v^2}$	$\frac{\overline{w_c^2}(z)}{v^2}$	$\frac{\Phi_{w_c}(\omega)}{v^2 L^3 / U}$
1	$\frac{1 - e^{-\beta}}{\beta}$	$\frac{\beta}{\beta^2} \left[\tilde{K}_1 \left(\sigma, \sinh^{-1} \frac{\beta}{\sigma} \right) - \sigma \tilde{K}_0 \left(\sigma, \sinh^{-1} \frac{\beta}{\sigma} \right) + \frac{\beta}{\sigma} \left(e^{-\sigma} - e^{-\sqrt{\sigma^2 + \beta^2}} \right) \right]$	$\frac{\beta}{\beta^2 (1 + k^2)^3} \left\{ 2k^2 \beta \sqrt{1 + k^2} K_0(\beta \sqrt{1+k^2}) + (1 - 2k^2) \left[2 - 2\beta \sqrt{1 + k^2} K_1(\beta \sqrt{1+k^2}) \right] - \beta^2 (1 + k^2) K_0(\beta \sqrt{1+k^2}) \right\}$
2	$\frac{\beta - \frac{1}{2}(1 - e^{-2\beta})}{\beta^2}$	$\frac{1}{\beta^2} \left[2\sigma \tilde{K}_1 \left(2\sigma, \sinh^{-1} \frac{\beta}{\sigma} \right) - (\sigma - 2\sigma - \sqrt{\sigma^2 + \beta^2} e^{-2\sqrt{\sigma^2 + \beta^2}}) - \frac{1}{2} \left(e^{-2\sigma} - e^{-2\sqrt{\sigma^2 + \beta^2}} \right) \right]$	$\frac{\beta}{\beta^2 (4 + k^2)^{3/2}} \left[K_0(\beta \sqrt{4+k^2}) + 2 K_1(\beta \sqrt{4+k^2}) - \frac{2}{\beta \sqrt{4+k^2}} \right]$
3	$\frac{1}{\beta} \operatorname{erf} \left(\frac{\sqrt{\pi}}{2} \beta \right)$	$\frac{1}{\beta} \left[\left(1 - \frac{\pi}{2} \sigma^2 \right) \operatorname{erf} \left(\frac{\sqrt{\pi}}{2} \beta \right) + \frac{\pi \sigma^2}{\beta} \left(1 - e^{-\frac{\pi}{4} \beta^2} \right) \right] e^{-\frac{\pi}{4} \sigma^2}$	$\frac{4}{\pi \beta^2} \left[k^2 \operatorname{erf} \left(\frac{\sqrt{\pi}}{2} \beta \right) + \left(1 - \frac{2}{\pi} k^2 \right) \left(1 - e^{-\frac{\pi}{4} \beta^2} \right) \right] e^{-\frac{k^2 R}{\pi}}$
4	$\frac{\beta \operatorname{erf}(\sqrt{\pi} \beta) - \frac{1}{2}(1 - e^{-\pi \beta^2})}{\beta^2}$	$\frac{\beta \operatorname{erf}(\sqrt{\pi} \beta) - \frac{1}{2}(1 - e^{-\pi \beta^2})}{\beta^2} e^{-\pi \sigma^2}$	$\frac{1}{\pi} \frac{\beta \operatorname{erf}(\sqrt{\pi} \beta) - \frac{1}{2}(1 - e^{-\pi \beta^2})}{\beta^2} e^{-\frac{k^2 R}{\pi}}$
5	Evaluated numerically	Evaluated numerically for $\beta = 0.5$	Evaluated numerically for $\beta = 0.5$
6	Same as case 1, plus: $\frac{1}{\beta C^2} [1 - (1 + C\beta)e^{-C\beta}]$	Same as case 1, plus: $\frac{\sigma}{C\beta} (1 - C^2 \sigma^2) \tilde{K}_1 \left(C\sigma, \sinh^{-1} \frac{\beta}{\sigma} \right) + \frac{2\sigma^2}{\beta} K_0 \left(C\sigma, \sinh^{-1} \frac{\beta}{\sigma} \right) + \frac{K_1^2}{\beta^2} e^{-C\sigma} - \left(\frac{1}{\beta} + \frac{\sigma^2}{\beta^2} \sqrt{\sigma^2 + \beta^2} \right) e^{-C \sqrt{\sigma^2 + \beta^2}}$	Same as case 1, plus: $\frac{2}{\pi} \frac{1}{\beta (C^2 + k^2)^{3/2}} \left\{ 2k^2 (k^2 C^2 - k^2) K_0(\beta \sqrt{C^2 + k^2}) - 3C^2 (C^2 + k^2) \beta \sqrt{C^2 + k^2} K_0(\beta \sqrt{C^2 + k^2}) - \left[C^4 \beta^2 (C^2 + k^2) + 6C^4 - 36C^2 k^2 + 6k^4 \right] K_1(\beta \sqrt{C^2 + k^2}) + \frac{6C^4 - 36C^2 k^2 + 6k^4}{\beta \sqrt{C^2 + k^2}} \right\}$

TABLE 6.-- AVERAGED CORRELATION FUNCTIONS AND POWER SPECTRA FOR
 LONGITUDINAL COMPONENT OF TURBULENCE
 [Rectangular loading; unswept wings]

Case	$\frac{v_{ue}(\xi)}{w^2}$	$\frac{\varphi_{ue}(\omega)}{w^2 L^* / U}$
1	$\frac{\sigma}{\beta} \tilde{K}_1\left(\sigma, \sinh^{-1} \frac{\beta}{\sigma}\right)$	$\frac{2}{\pi} \frac{1}{\beta(1+k'^2)^{3/2}} \left[K_1\left(\beta\sqrt{1+k'^2}\right) - \beta\sqrt{1+k'^2} K_0\left(\beta\sqrt{1+k'^2}\right) \right]$
3	$\frac{1}{\beta} \operatorname{erf}\left(\frac{\sqrt{\pi}}{2} \beta\right) e^{-\frac{\pi\sigma^2}{4}}$	$\frac{2}{\pi} \frac{1}{\beta} \operatorname{erf}\left(\frac{\sqrt{\pi}}{2} \beta\right) e^{-\frac{k'^2}{\pi}}$
6	Same as case 1, plus: $\frac{\sigma}{C\beta} \left[C\sigma \tilde{K}_0\left(C\sigma, \sinh^{-1} \frac{\beta}{\sigma}\right) + \tilde{K}_1\left(C\sigma, \sinh^{-1} \frac{\beta}{\sigma}\right) \right] -$ $\frac{1}{C} e^{-C\sqrt{\sigma^2+\beta^2}}$	Same as case 1, plus: $\frac{2}{\pi} \frac{1}{\beta(C^2+k'^2)^{5/2}} \left\{ (2C^2-k'^2) \left[K_1\left(\beta\sqrt{C^2+k'^2}\right) - \right. \right.$ $\left. \left. \beta\sqrt{C^2+k'^2} K_0\left(\beta\sqrt{C^2+k'^2}\right) \right] - C^2\beta^2(1+k'^2) K_1\left(\beta\sqrt{C^2+k'^2}\right) \right\}$

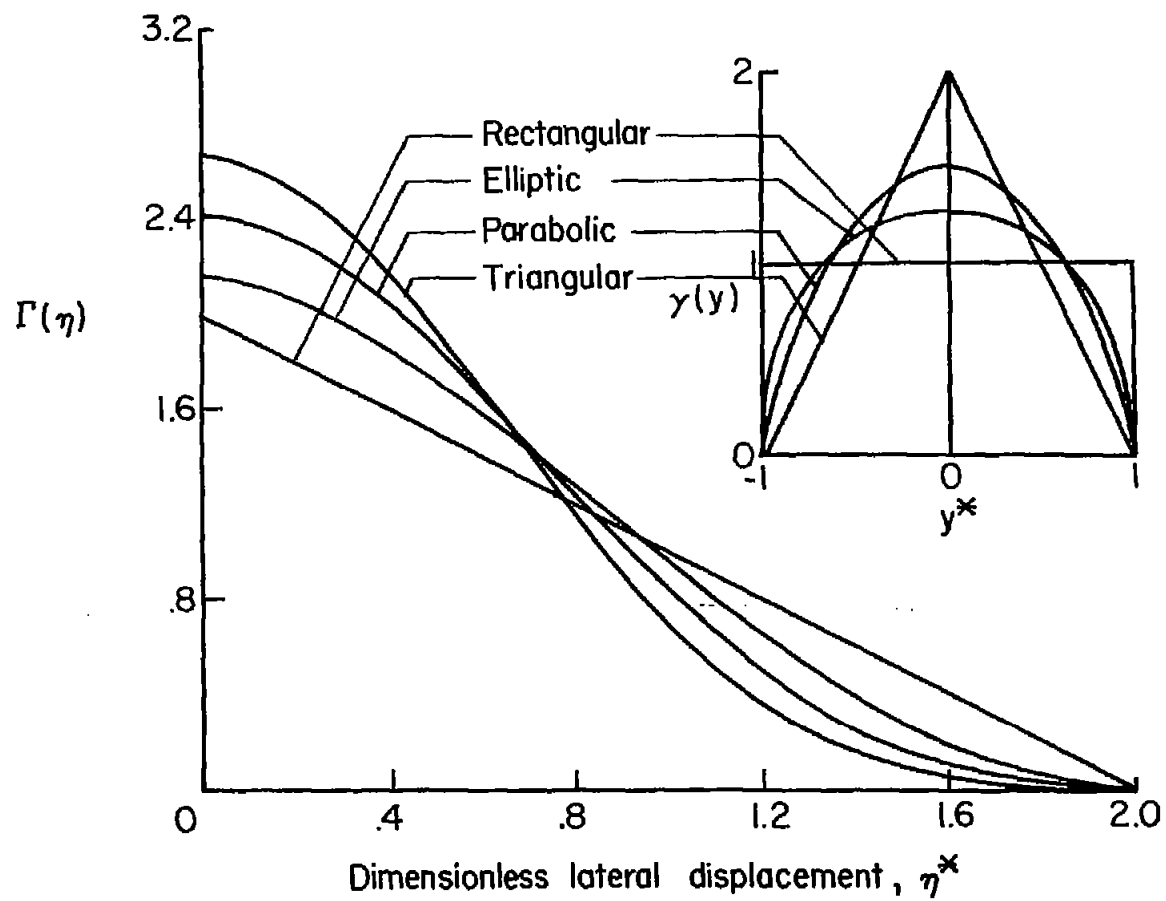
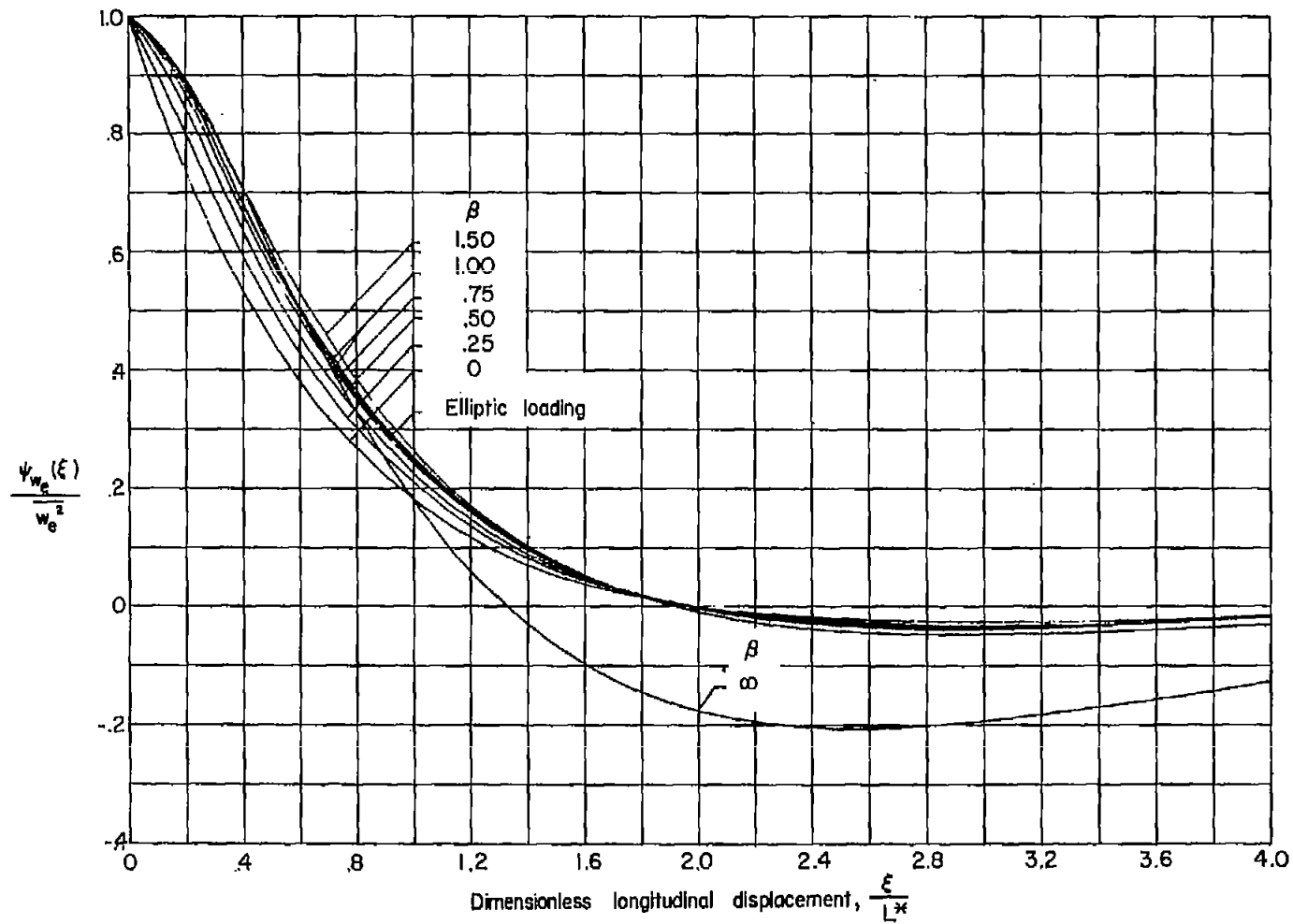
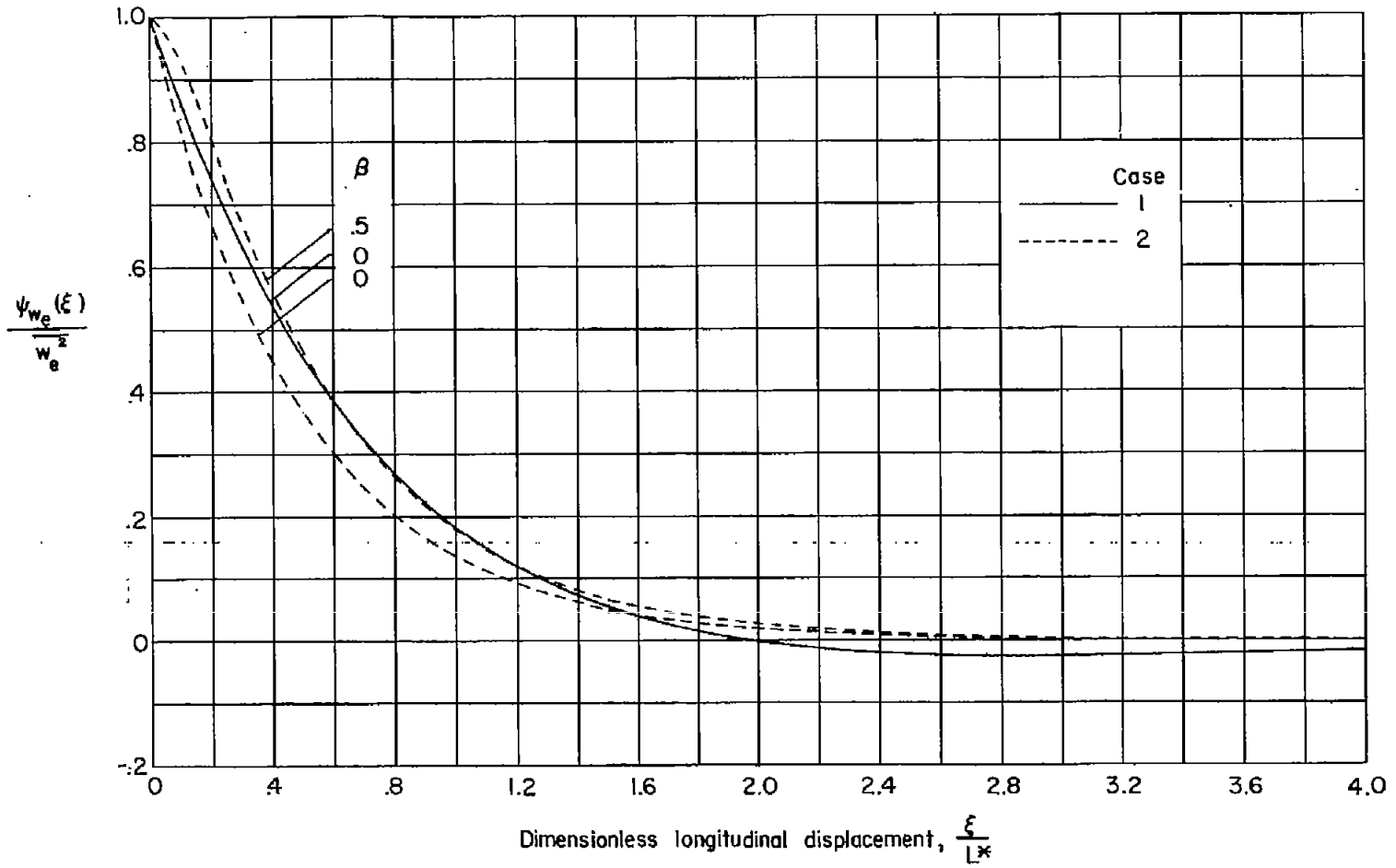


Figure 1.- Spanwise loading functions $\gamma(y)$ and corresponding functions $\Gamma(\eta)$ used in calculations.



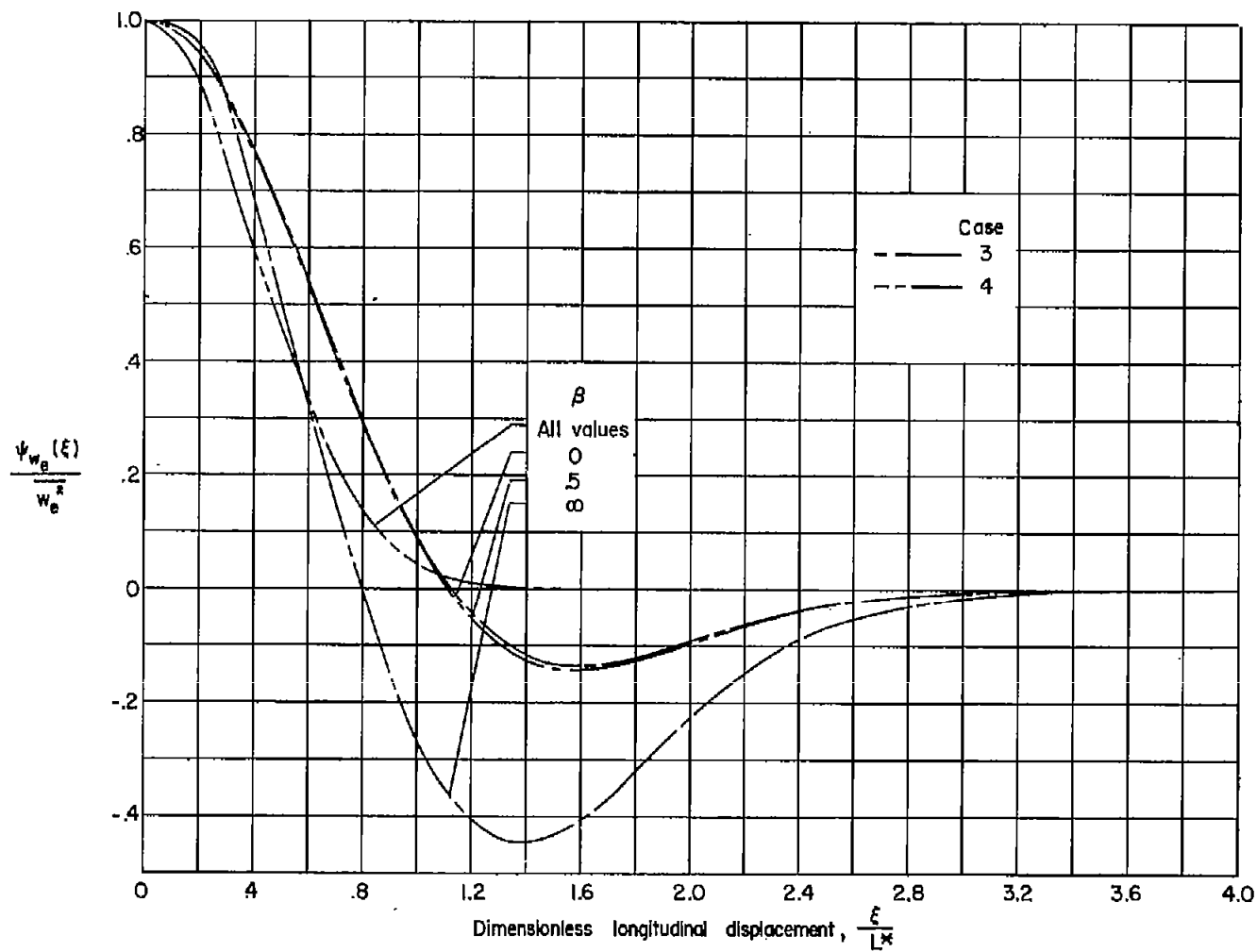
(a) Case 1.

Figure 2.- Point and averaged normal correlation functions for unswept wings with rectangular loading (unless specified otherwise).



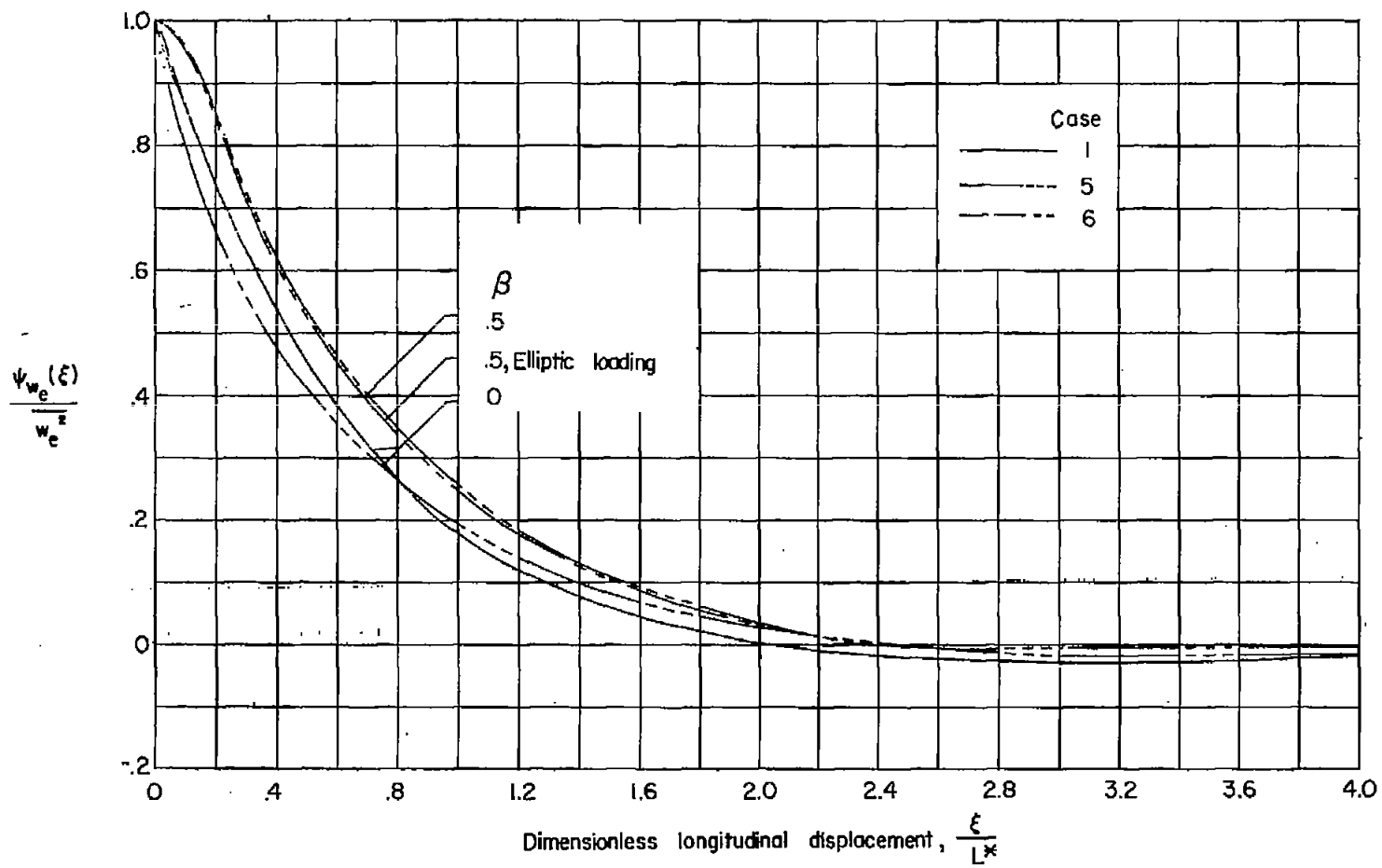
(b) Cases 1 and 2.

Figure 2.- Continued.



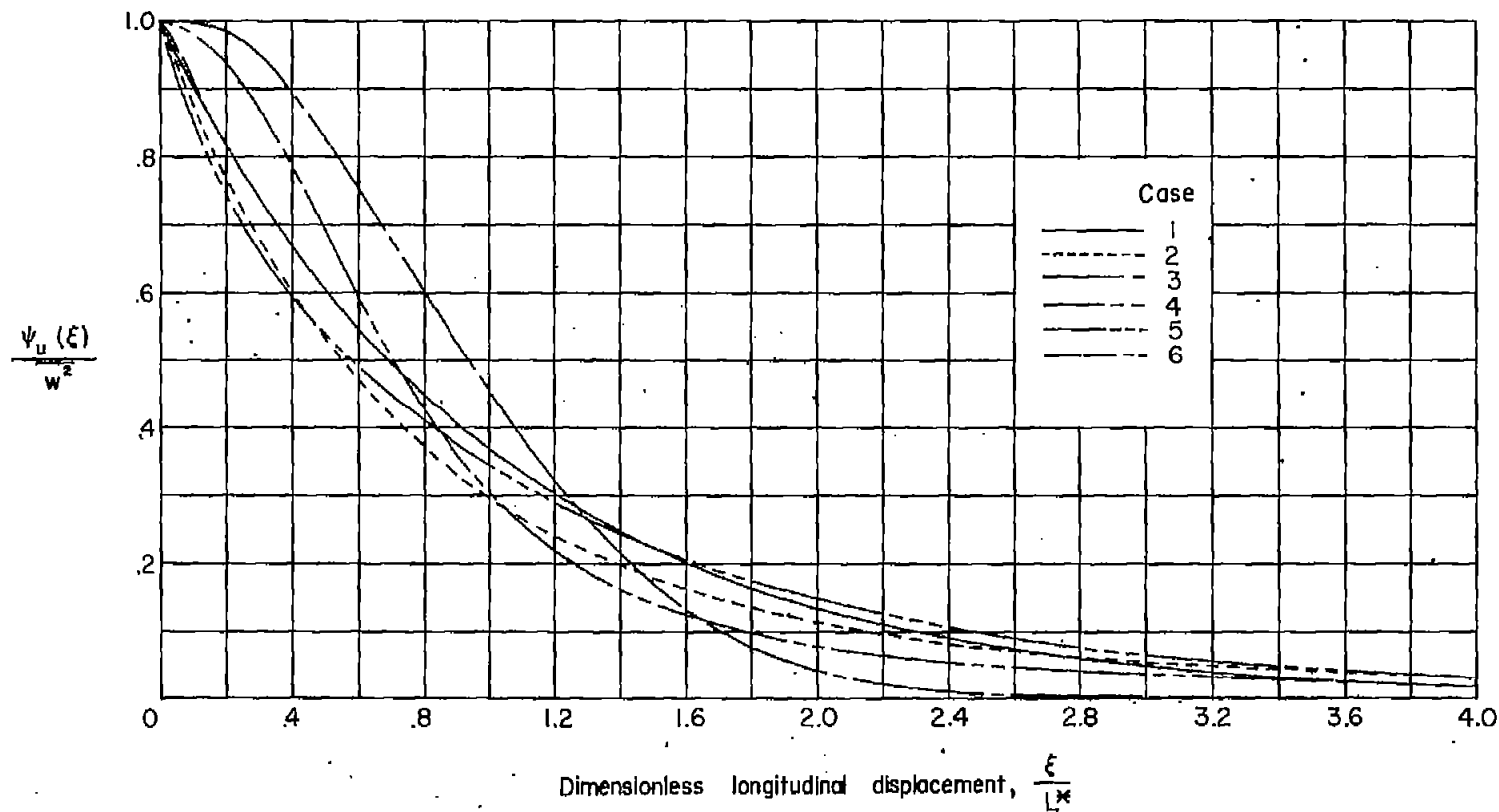
(c) Cases 3 and 4.

Figure 2.- Continued.



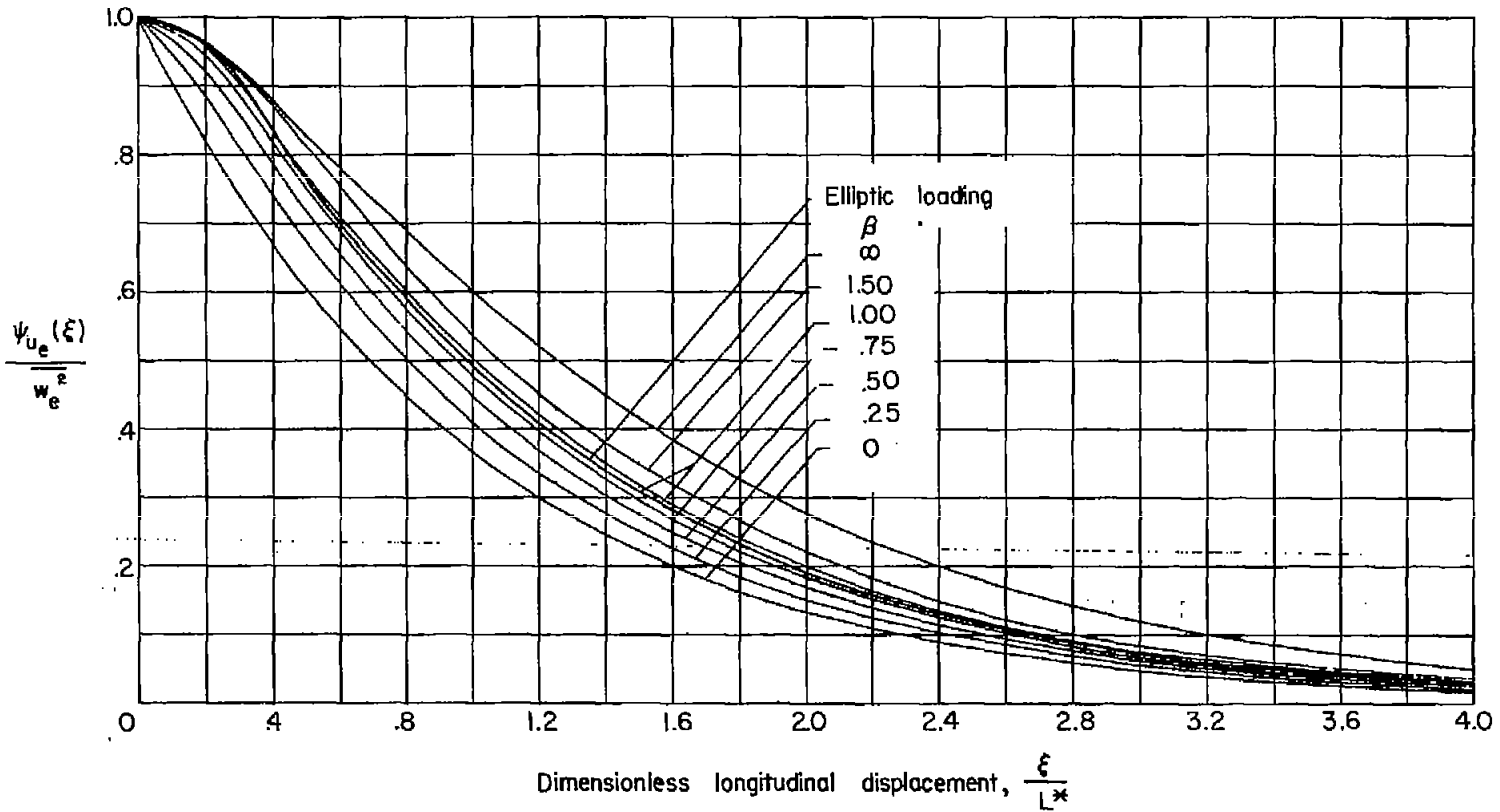
(d) Cases 5 and 6.

Figure 2.- Concluded.



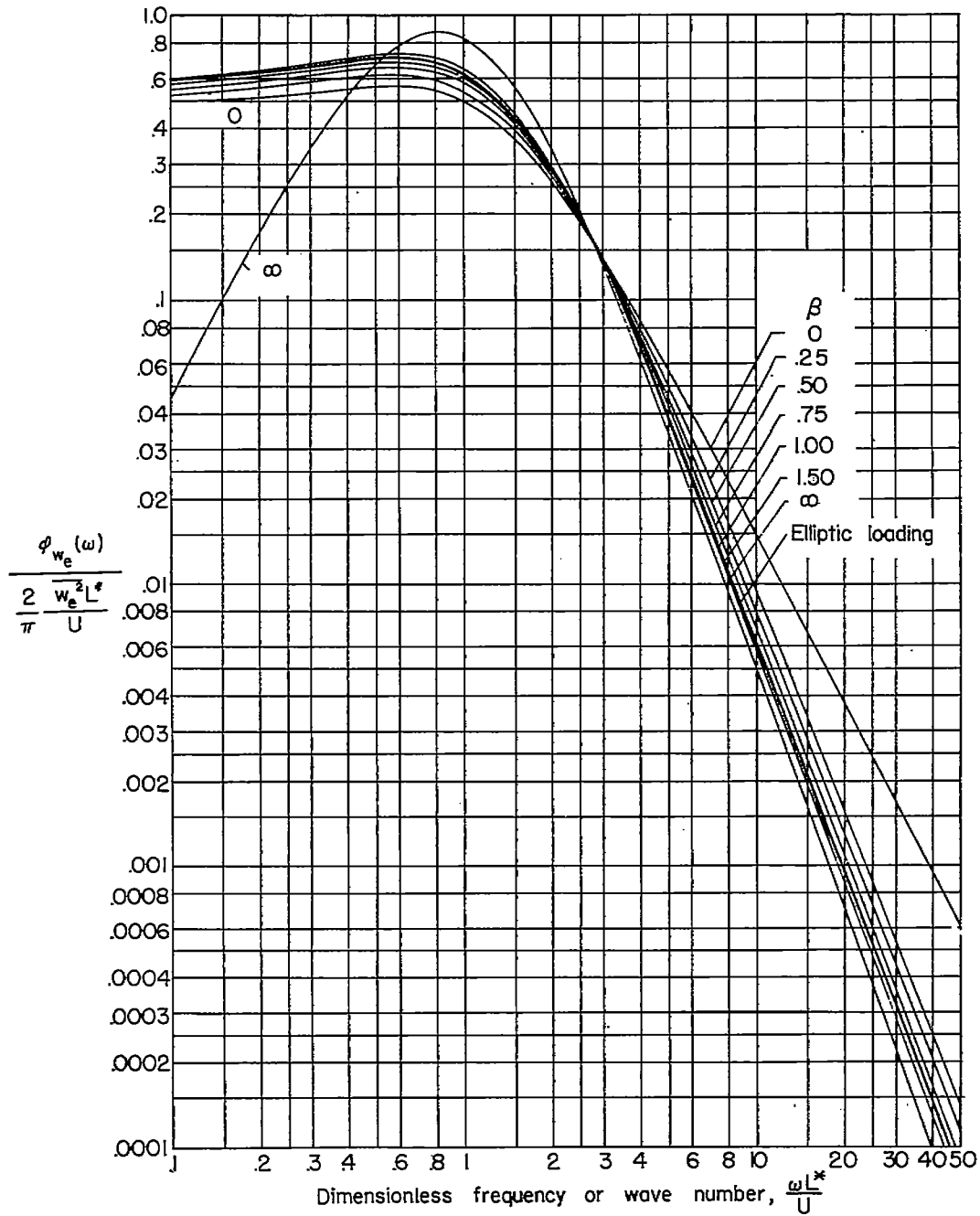
(a) Point correlation functions.

Figure 3.- Longitudinal correlation functions for unswept wings.



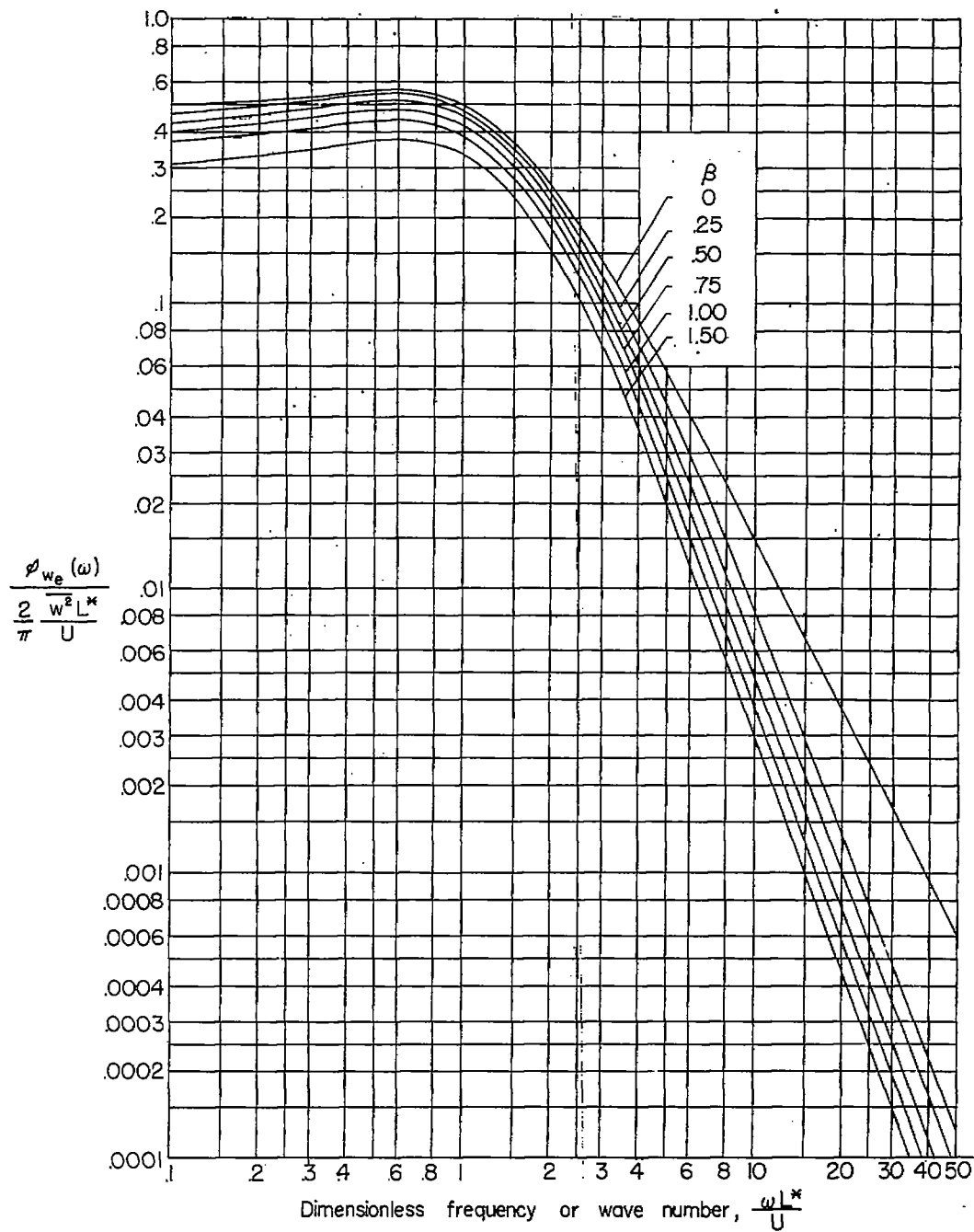
(b) Averaged correlation functions for case 1 for rectangular loading (unless specified otherwise).

Figure 3.- Concluded.



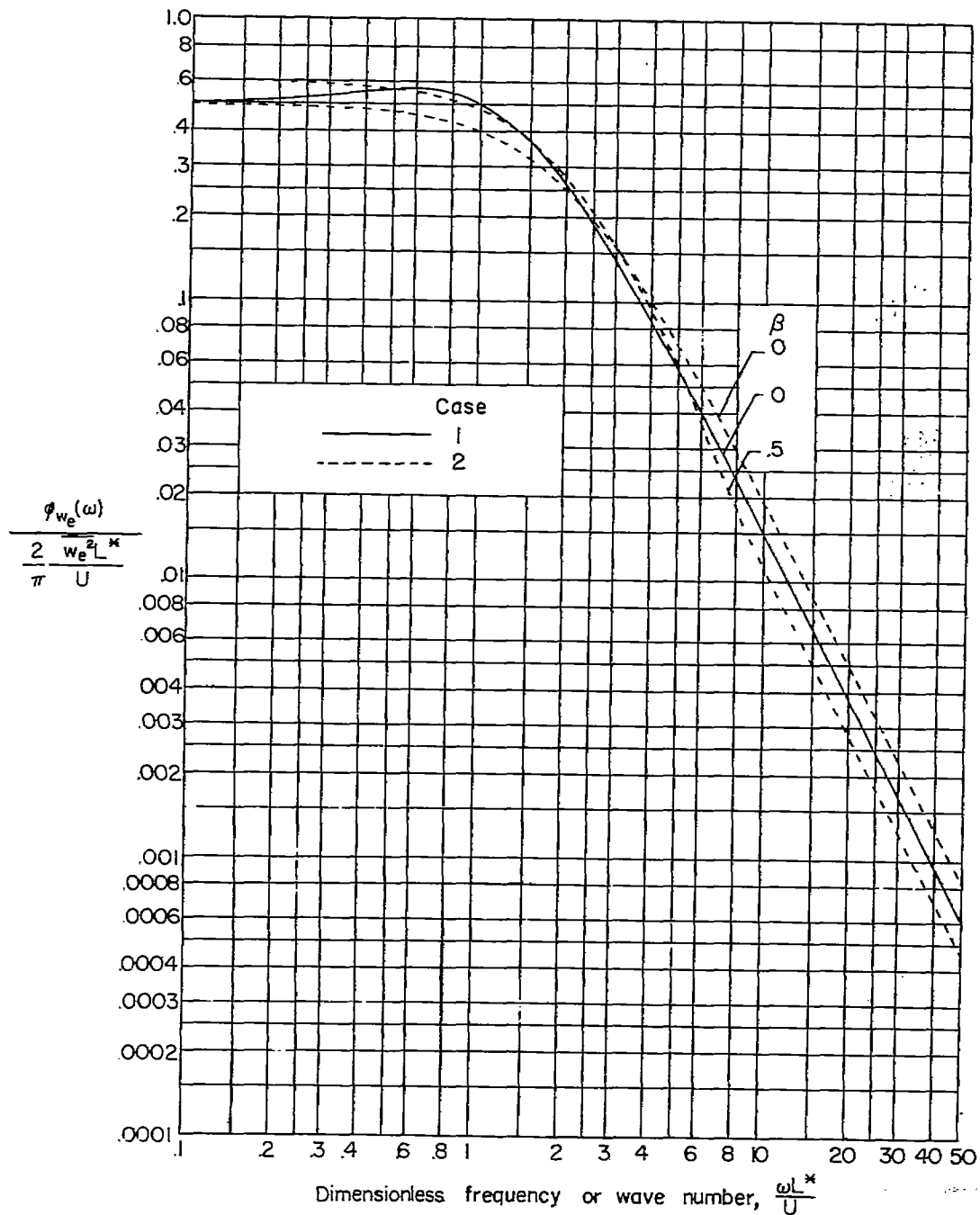
(a) Case 1.

Figure 4.- Point and averaged normal power spectra for unswept wings with rectangular loading (unless specified otherwise).



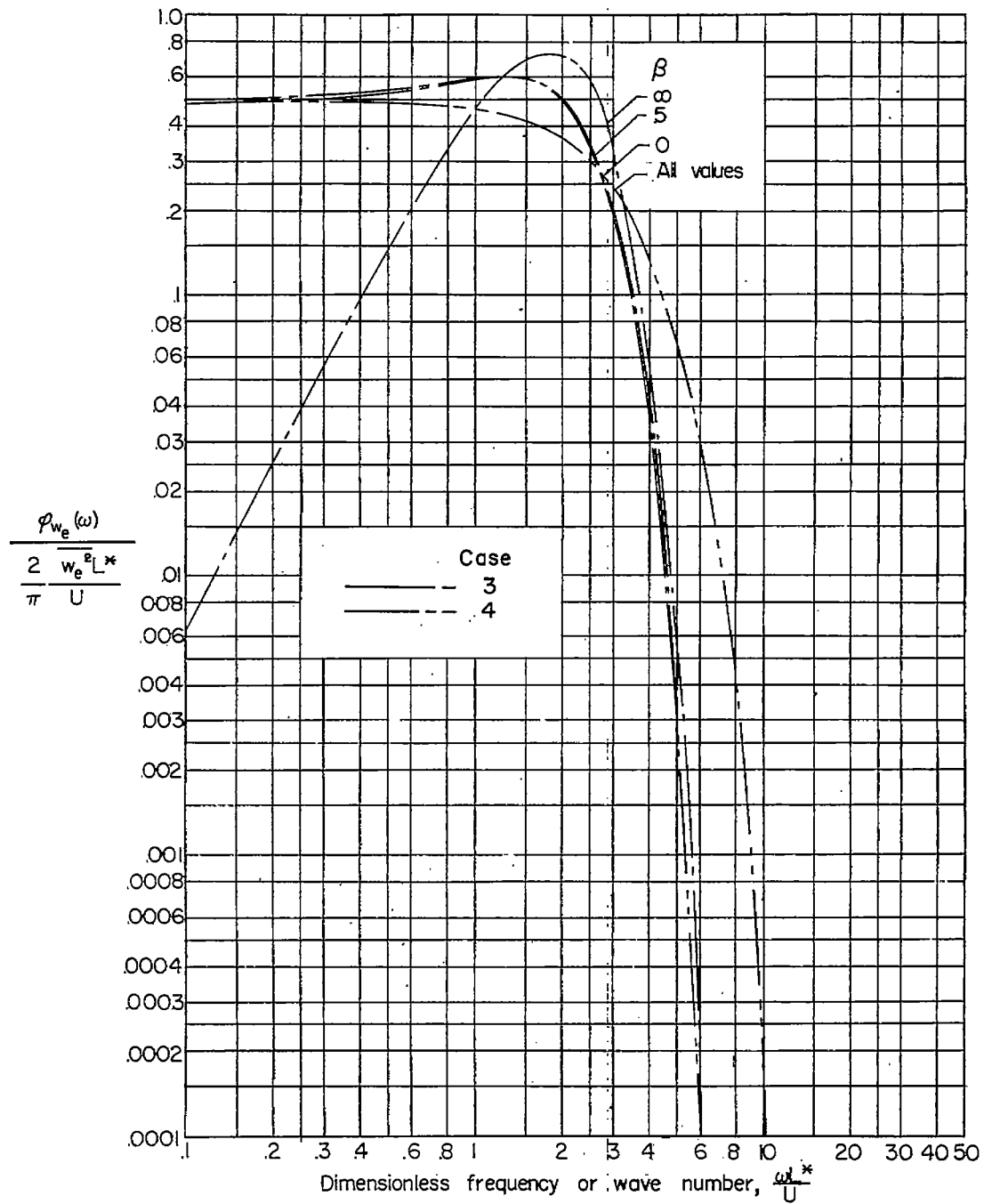
(b) Case 1; normalized with $\overline{w^2}$.

Figure 4.- Continued.



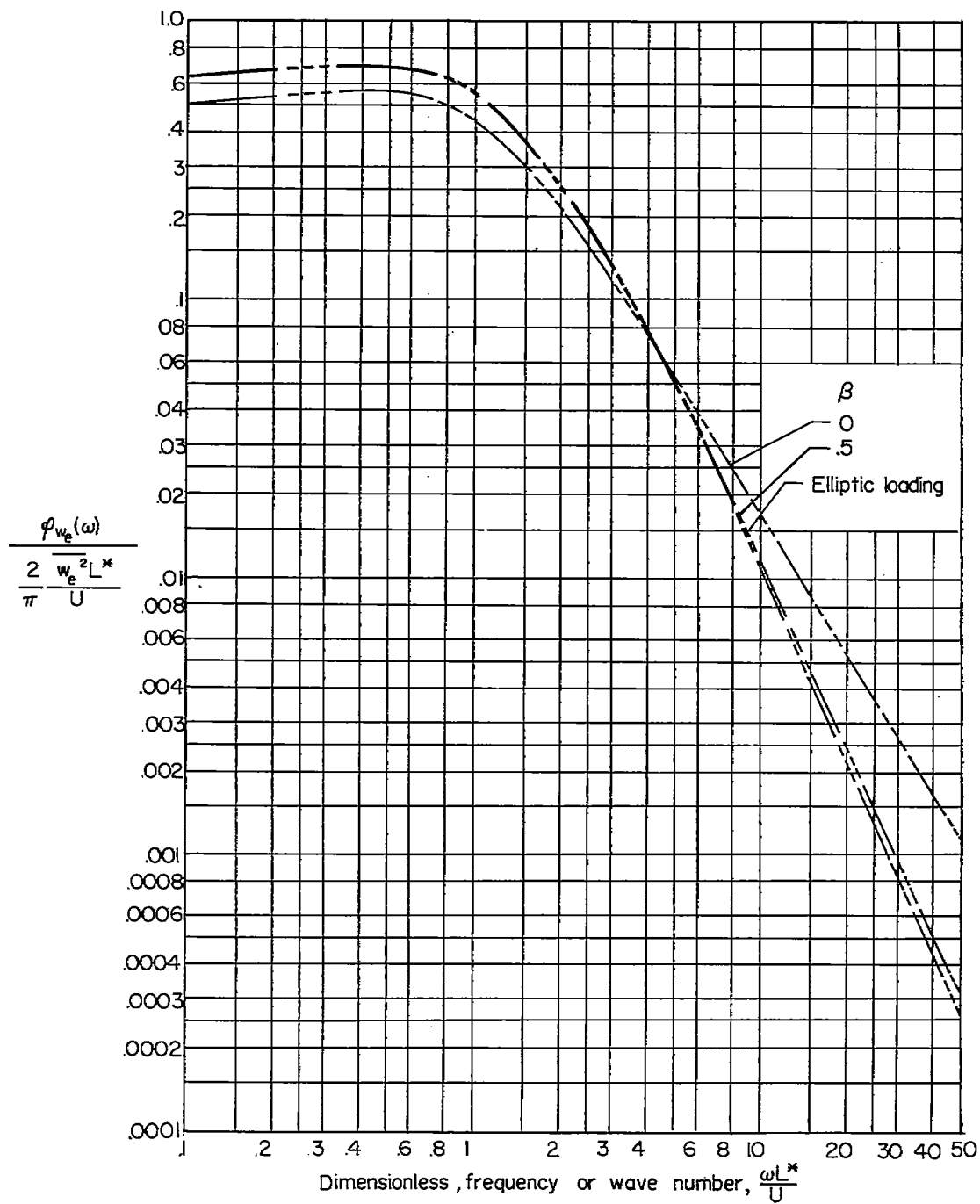
(c) Cases 1 and 2.

Figure 4.- Continued.



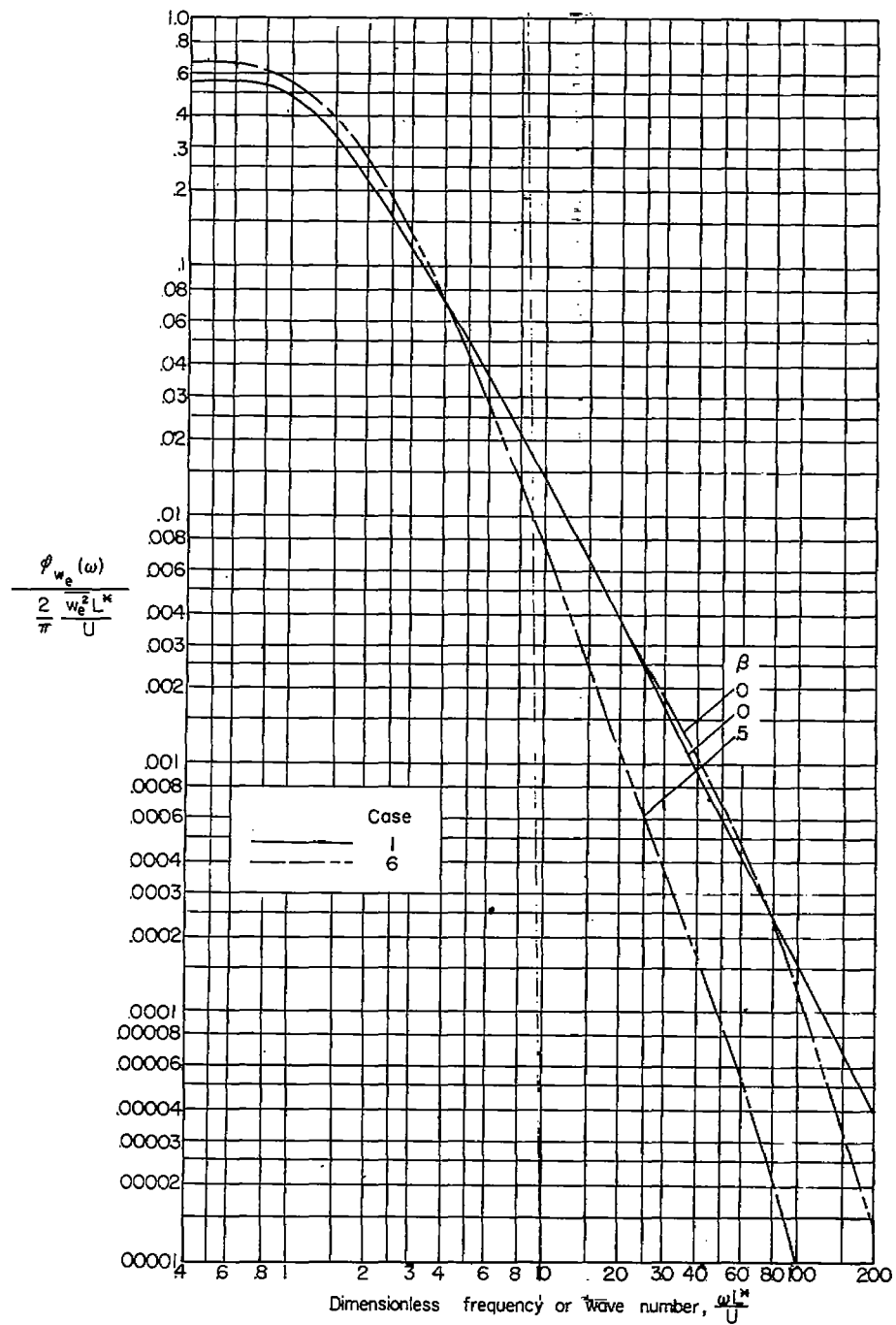
(d) Cases 3 and 4.

Figure 4.- Continued.



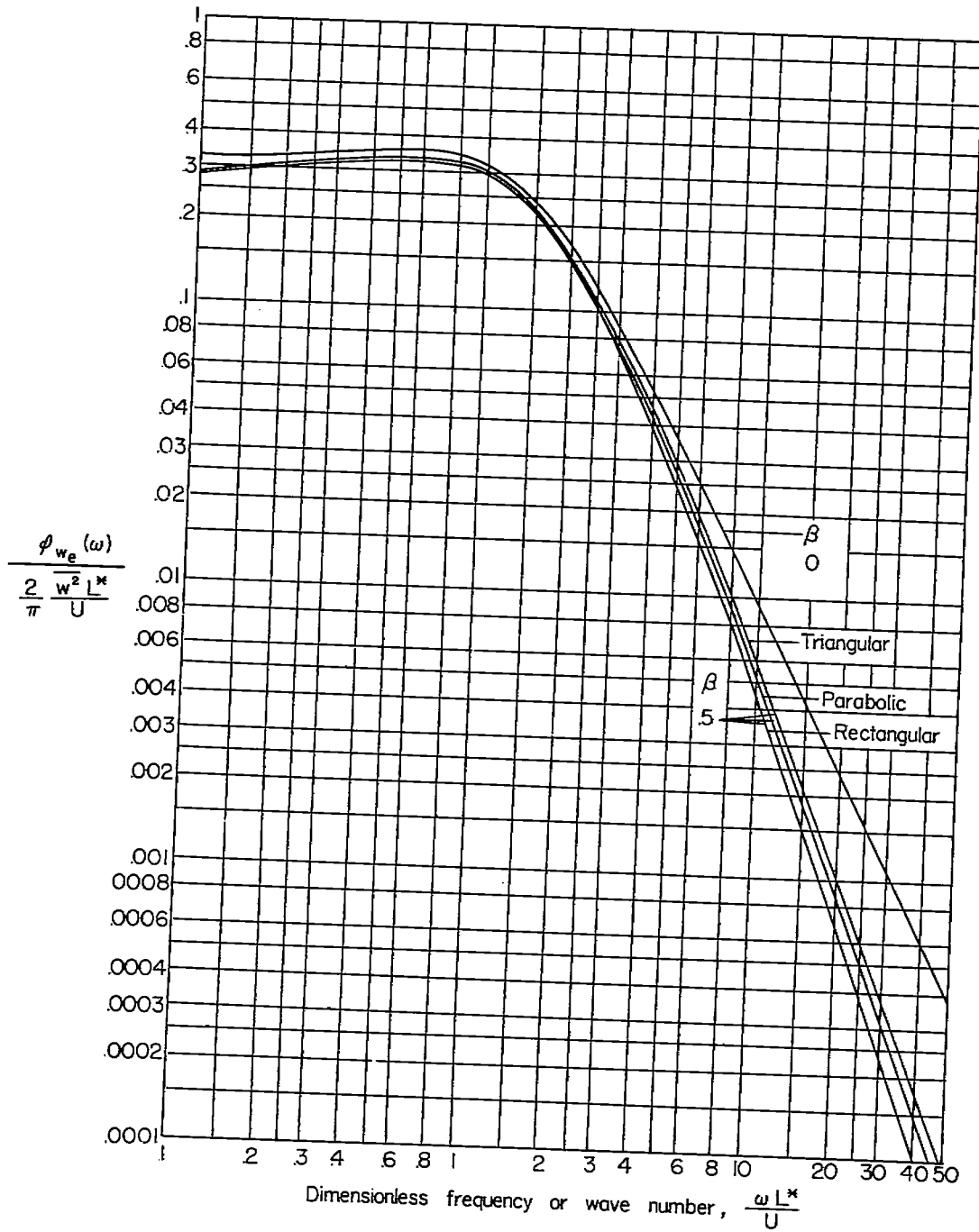
(e) Case 5.

Figure 4.- Continued.



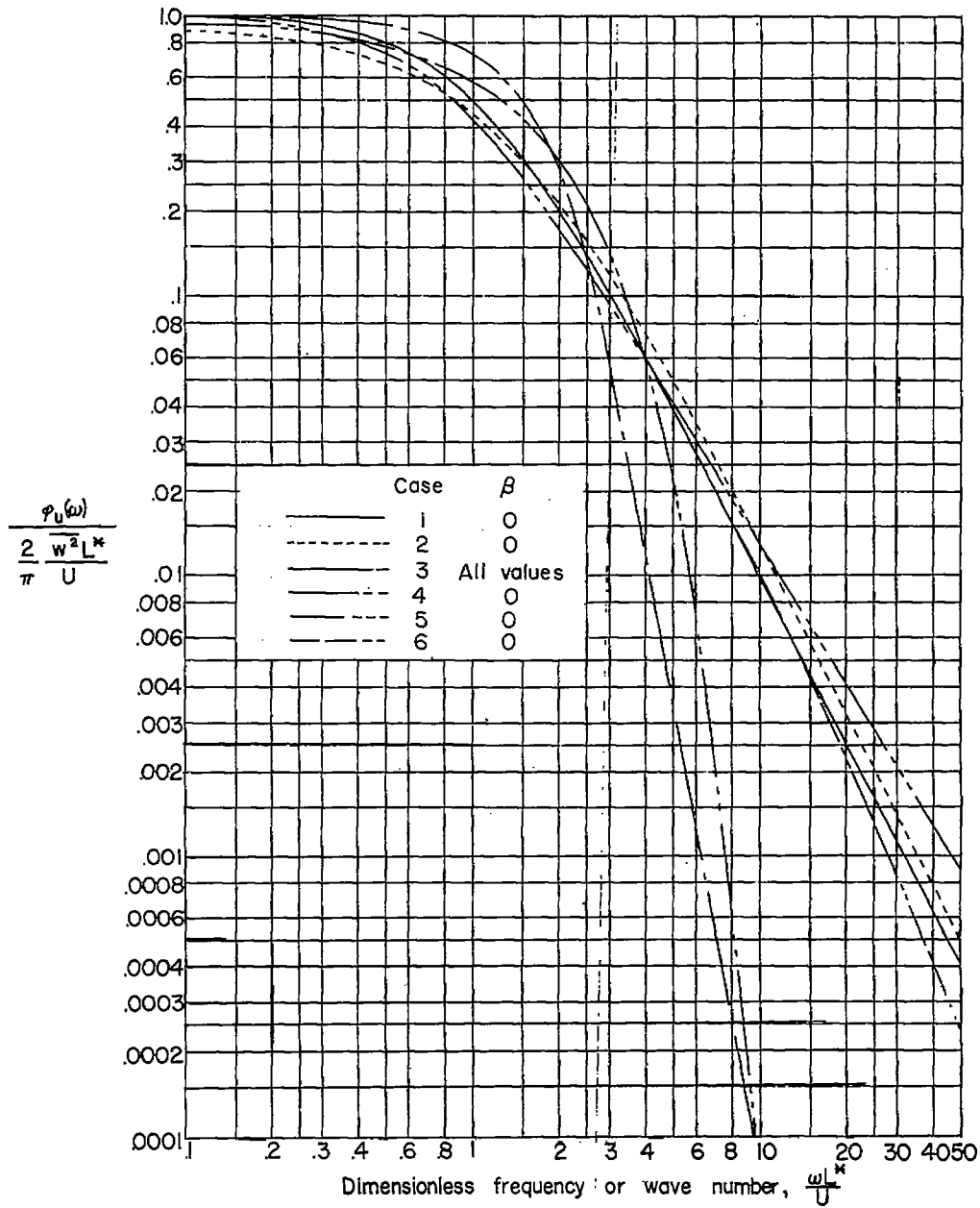
(f) Cases 1 and 6.

Figure 4.- Continued.



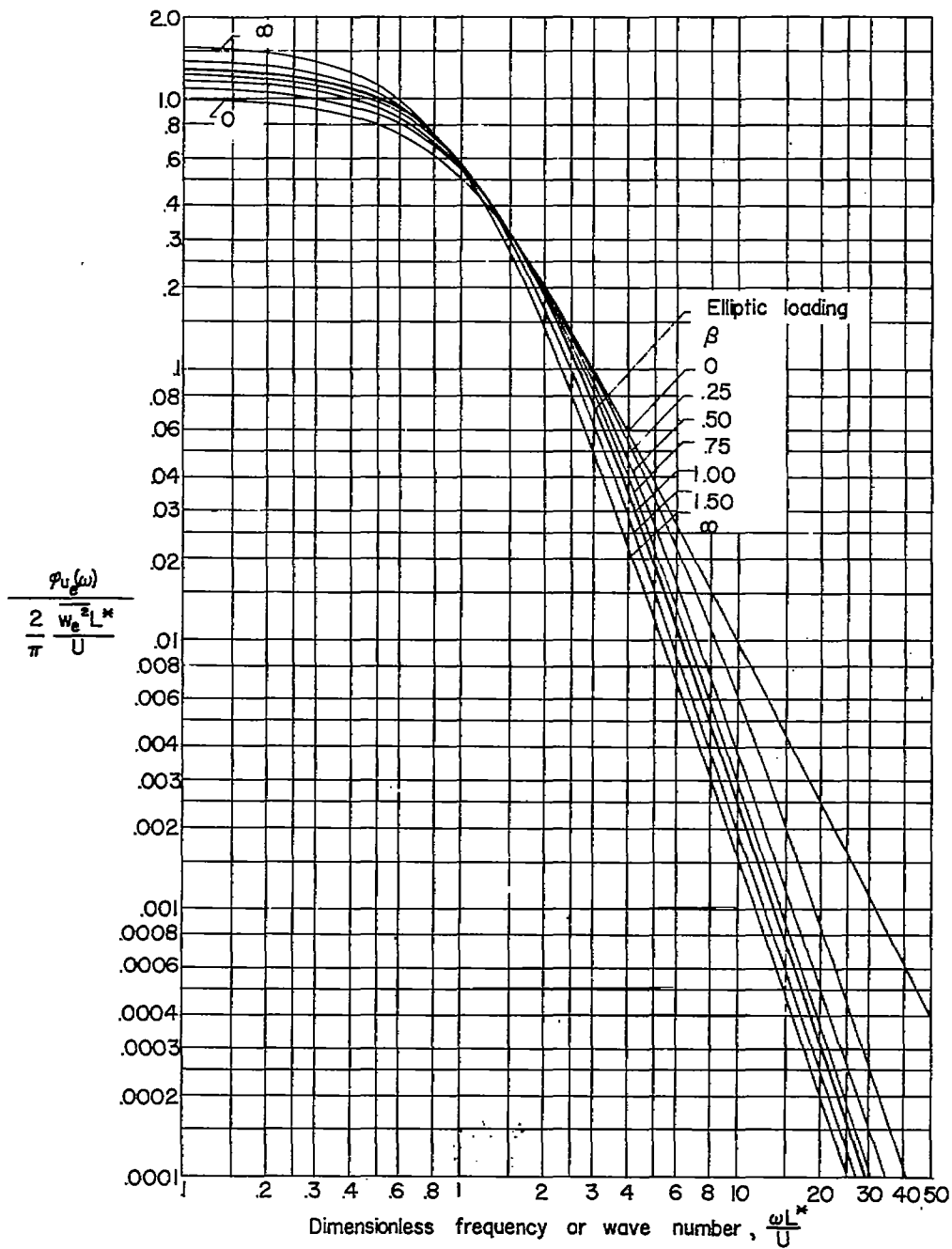
(g) Case 1; various loadings.

Figure 4.- Concluded.



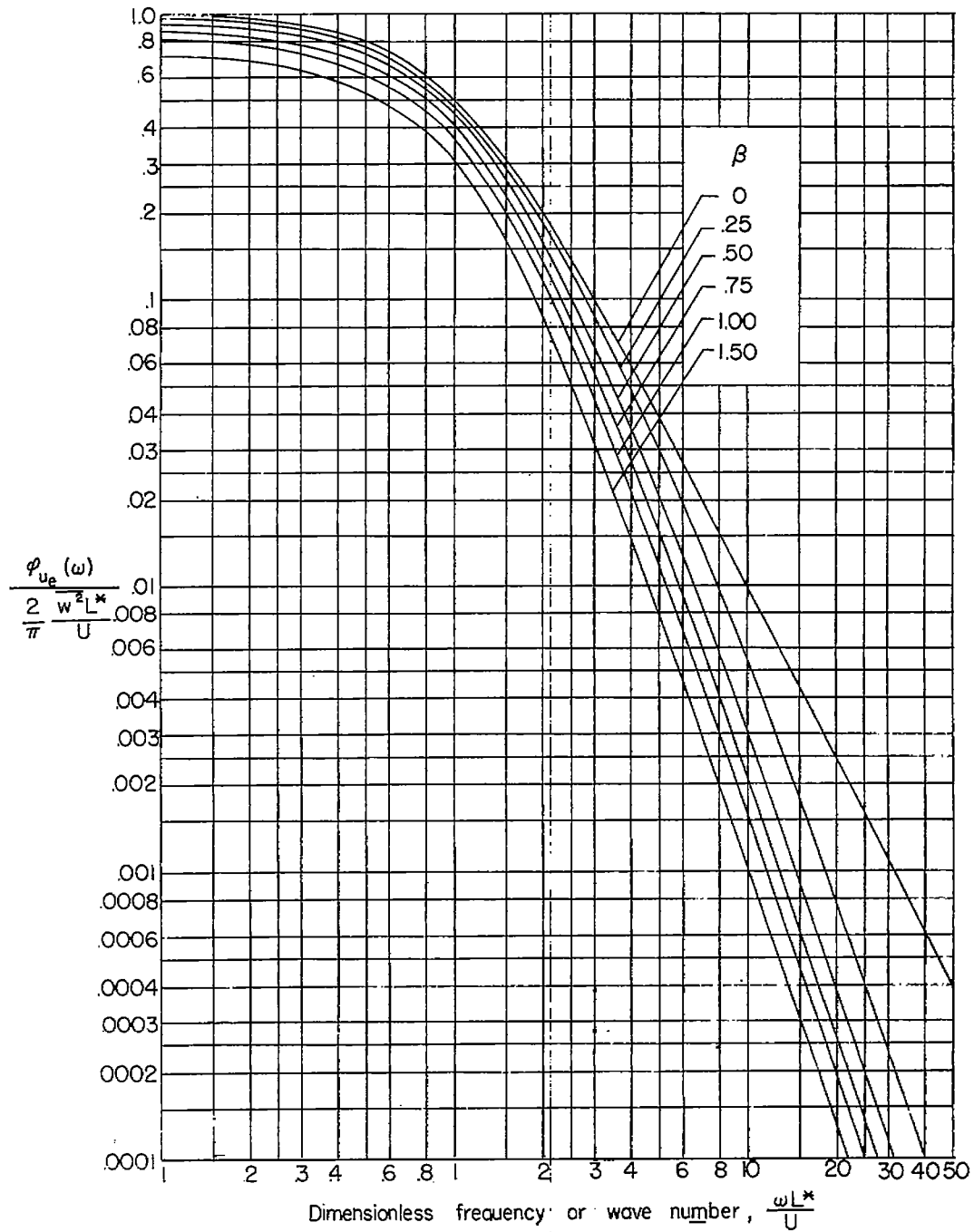
(a) Point spectra.

Figure 5.- Longitudinal power spectra for unswept wings.



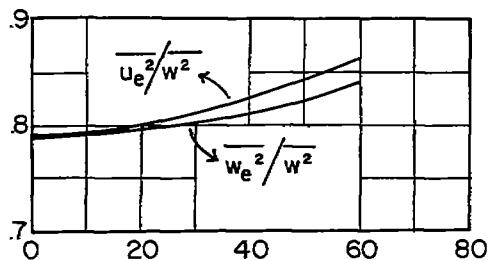
(b) Averaged spectra for case 1; rectangular loading (unless specified otherwise).

Figure 5.- Continued.



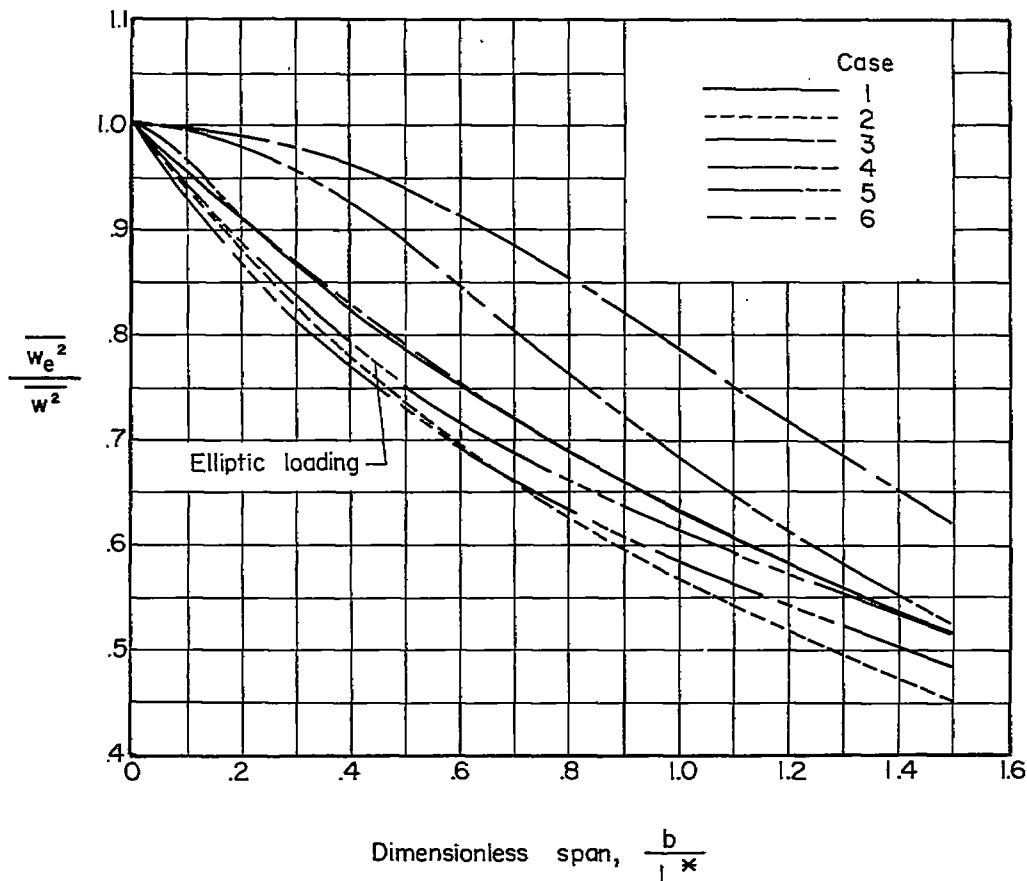
(c) Averaged spectra for case 1; rectangular loading; normalized with $\overline{w^2}$.

Figure 5.- Concluded.



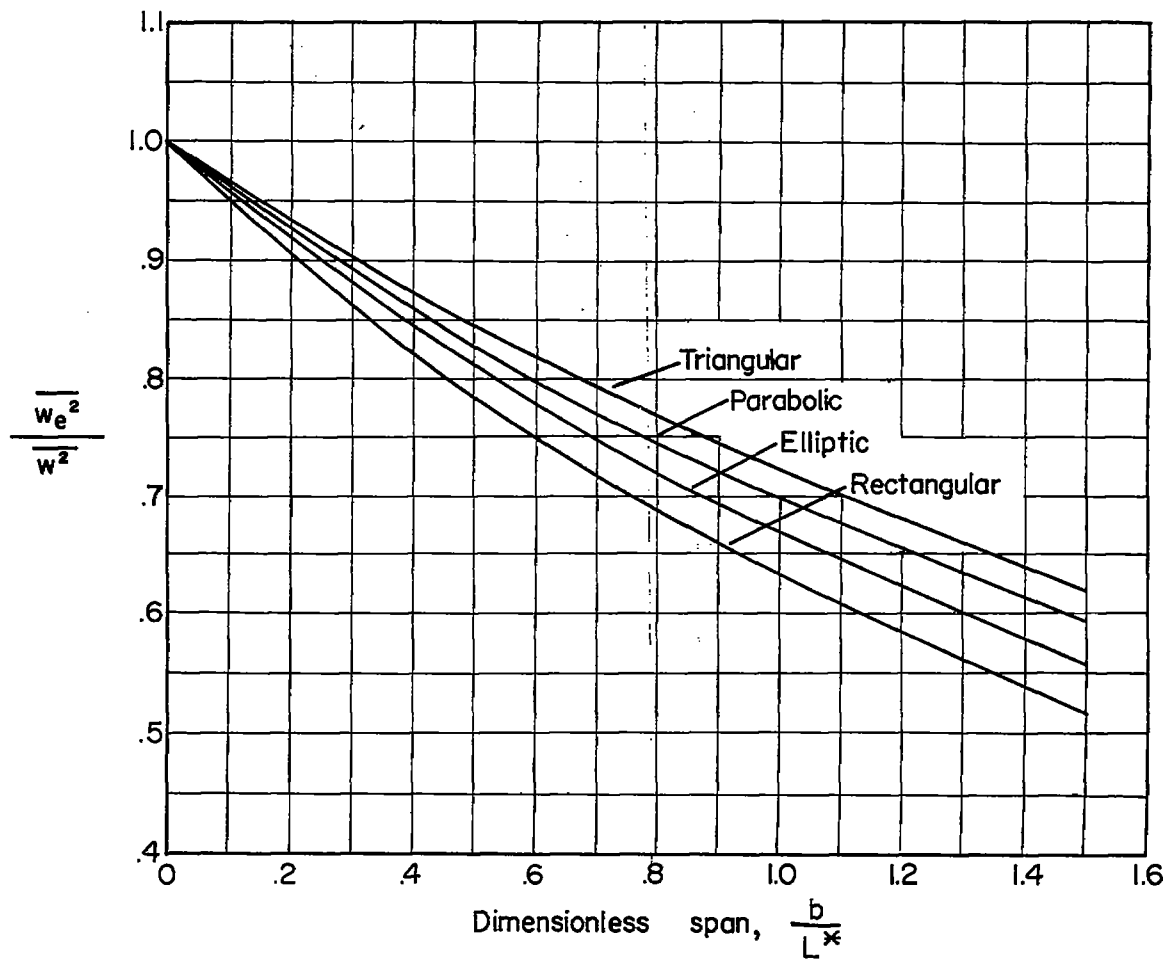
Angle of sweepback, Λ , deg

(a) Swept wings with rectangular loading and $\frac{b}{L^*} \cos \Lambda = 0.5$; case 1.



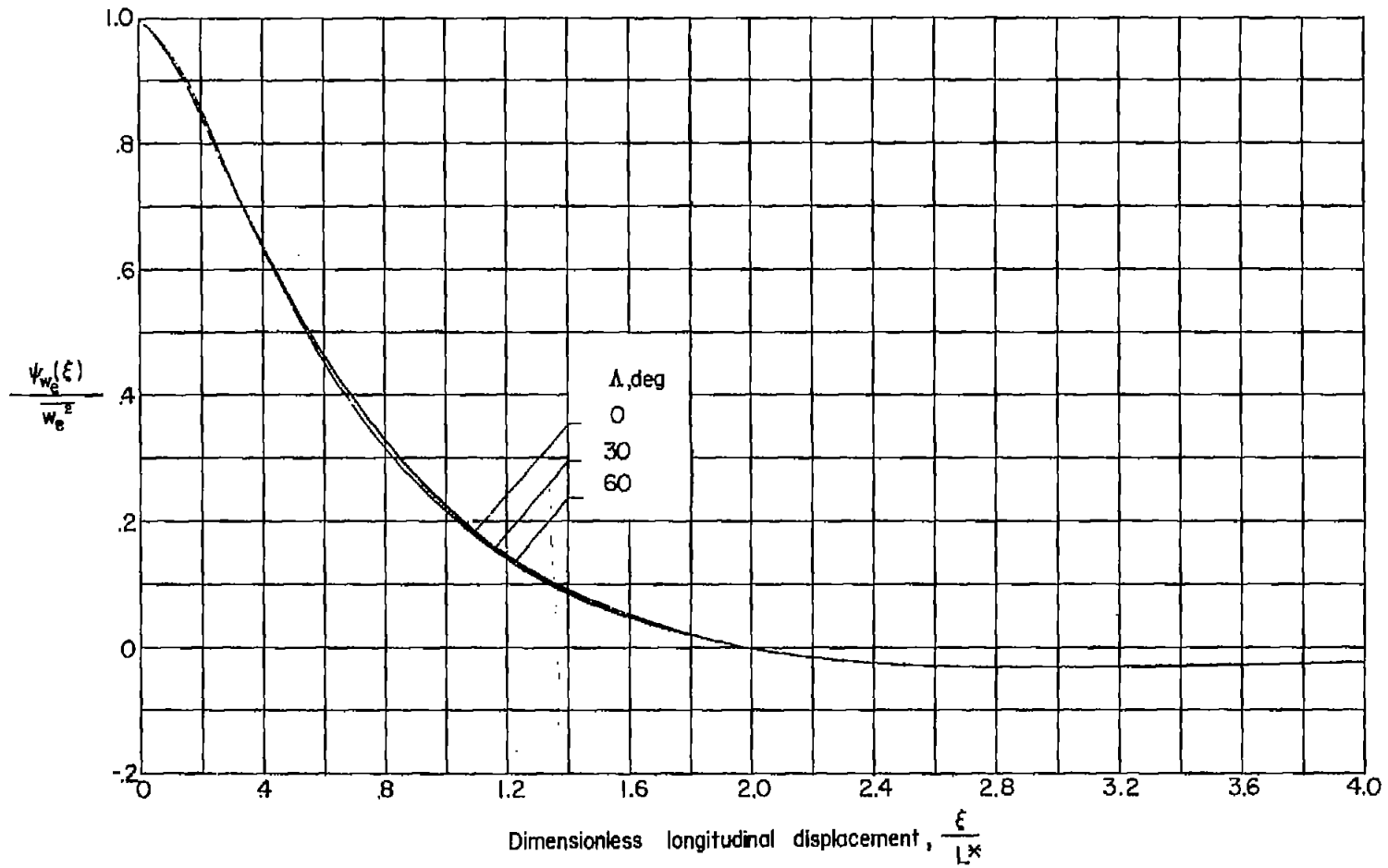
(b) Unswept wings with rectangular loadings (unless specified otherwise).

Figure 6.- Mean-square averaged intensity of turbulence.



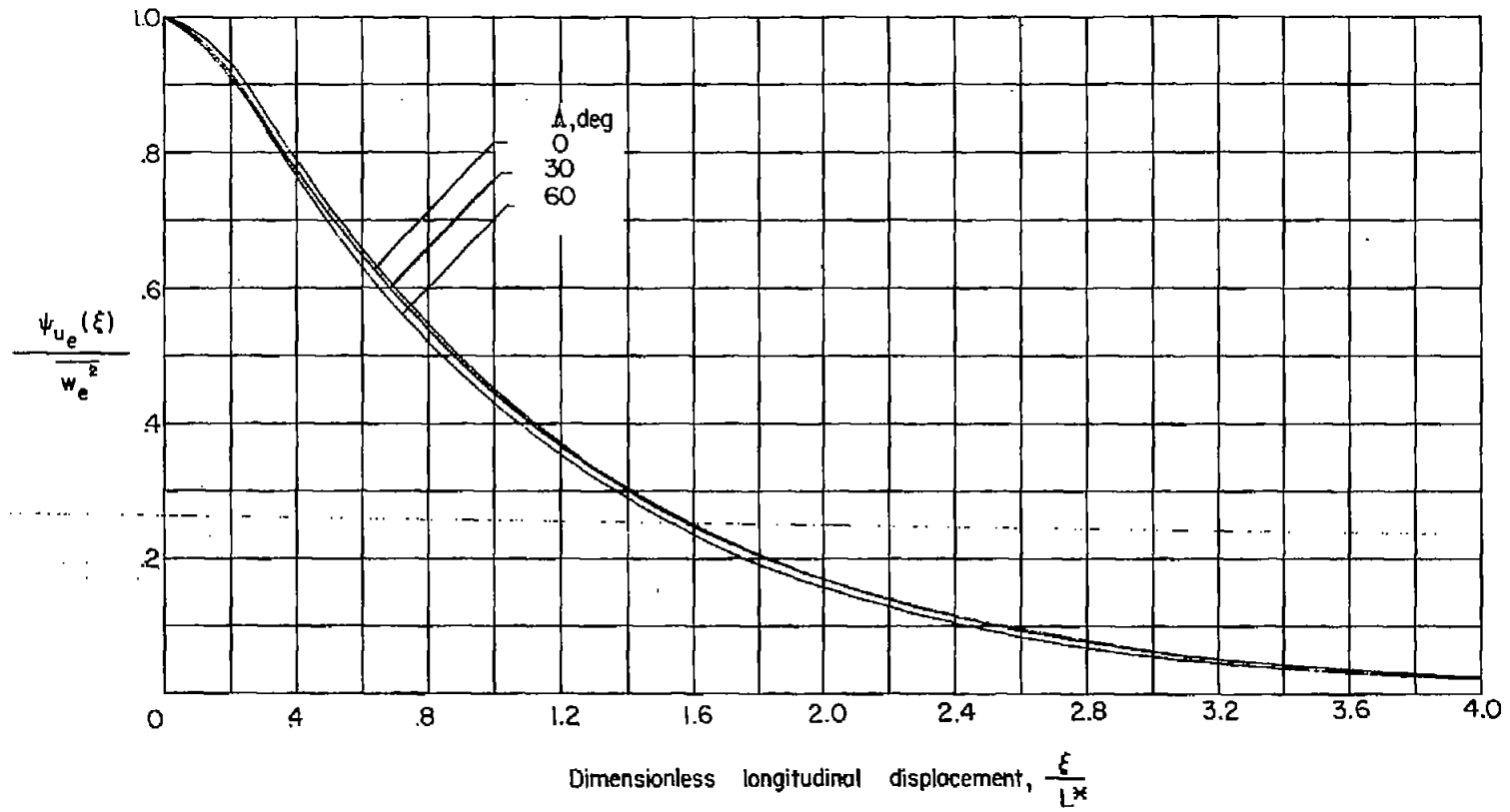
(c) Unswept wings with various loadings; case 1.

Figure 6.- Concluded.



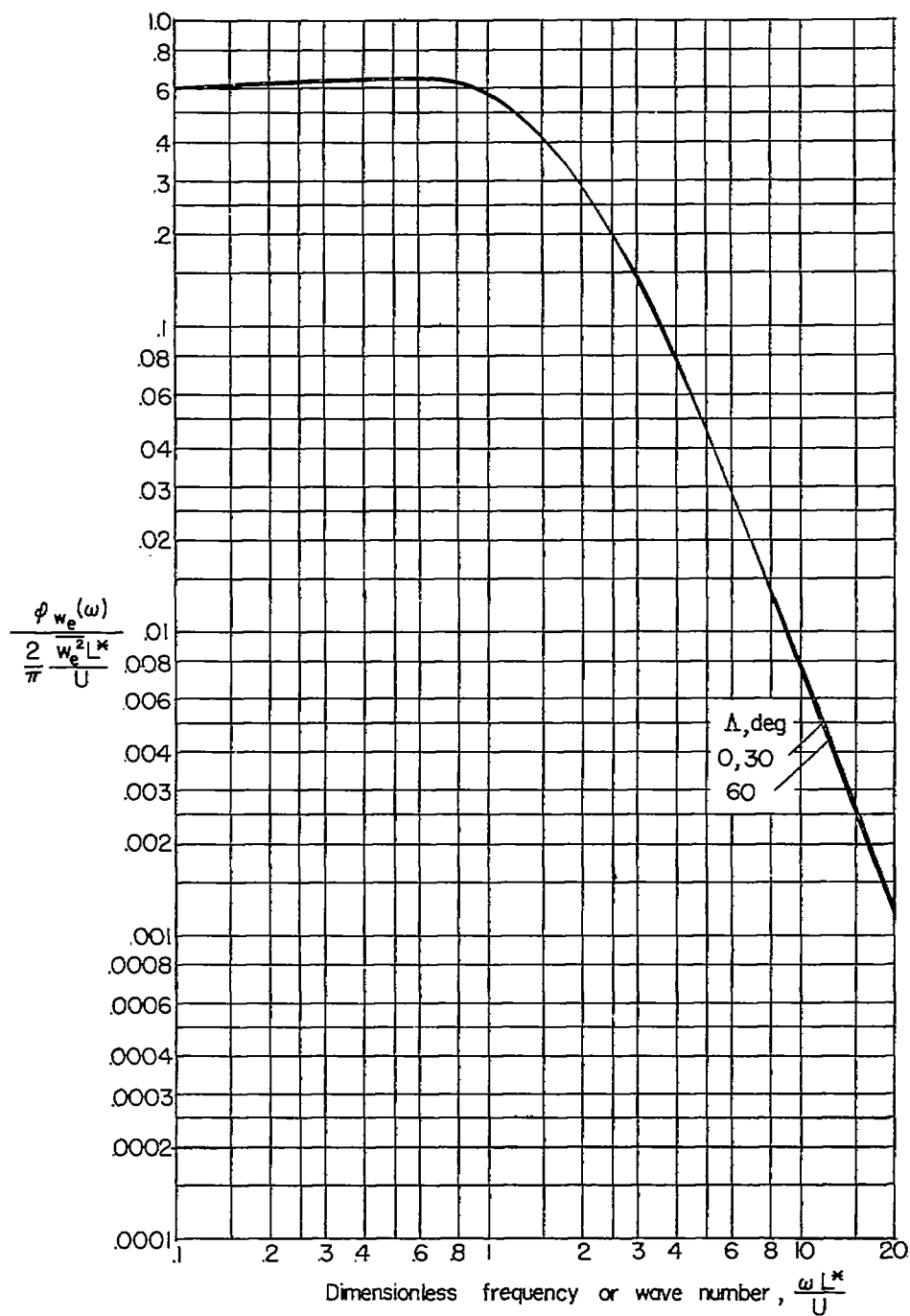
(a) Normal correlation functions.

Figure 7.- Averaged correlation functions and spectra for swept wings with rectangular loading and $\frac{b}{L^*} \cos \Lambda = 0.5$; case 1.



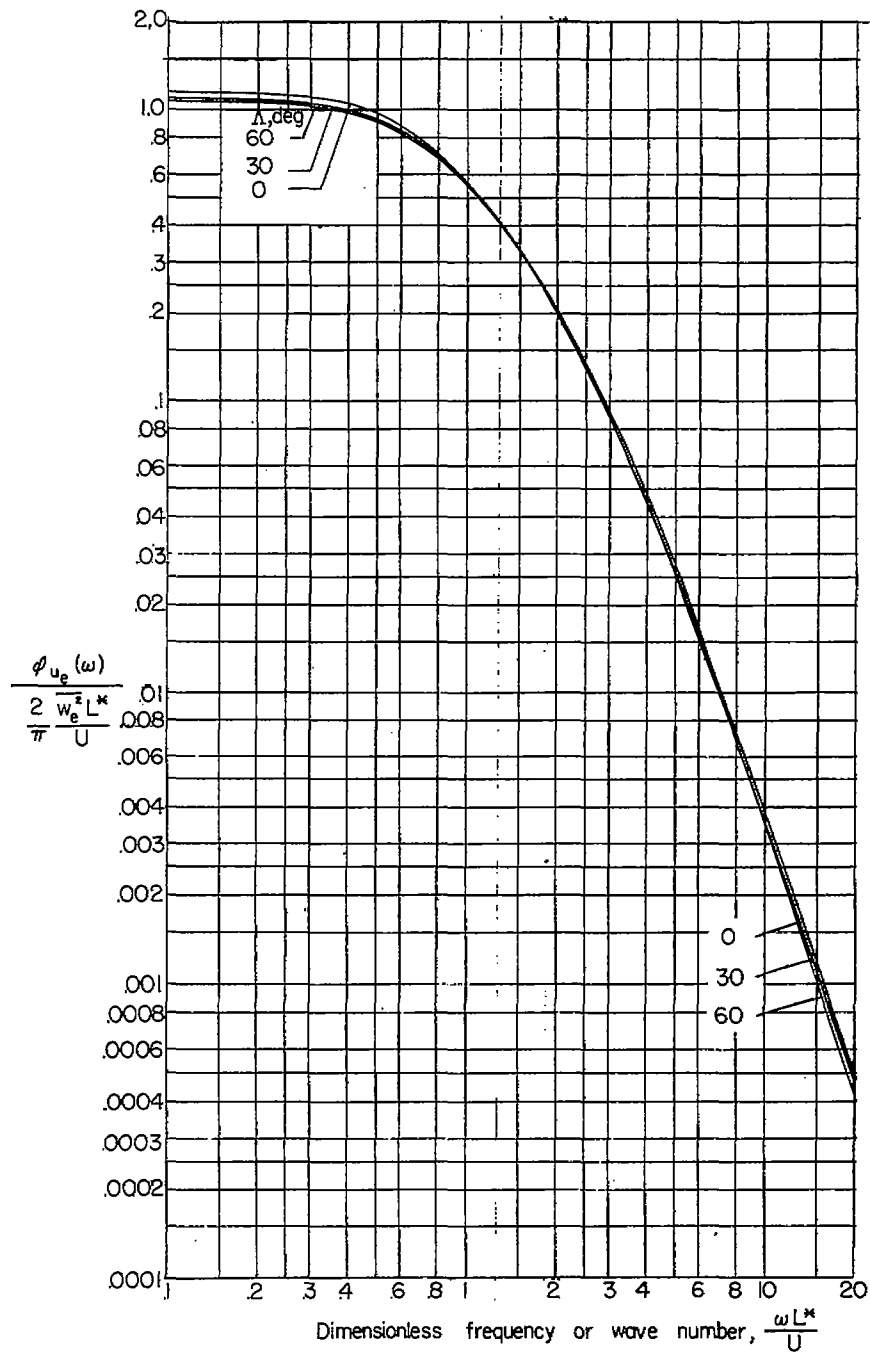
(b) Longitudinal correlation functions.

Figure 7.- Continued.



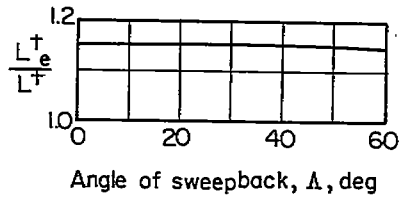
(c) Normal spectra.

Figure 7.- Continued.

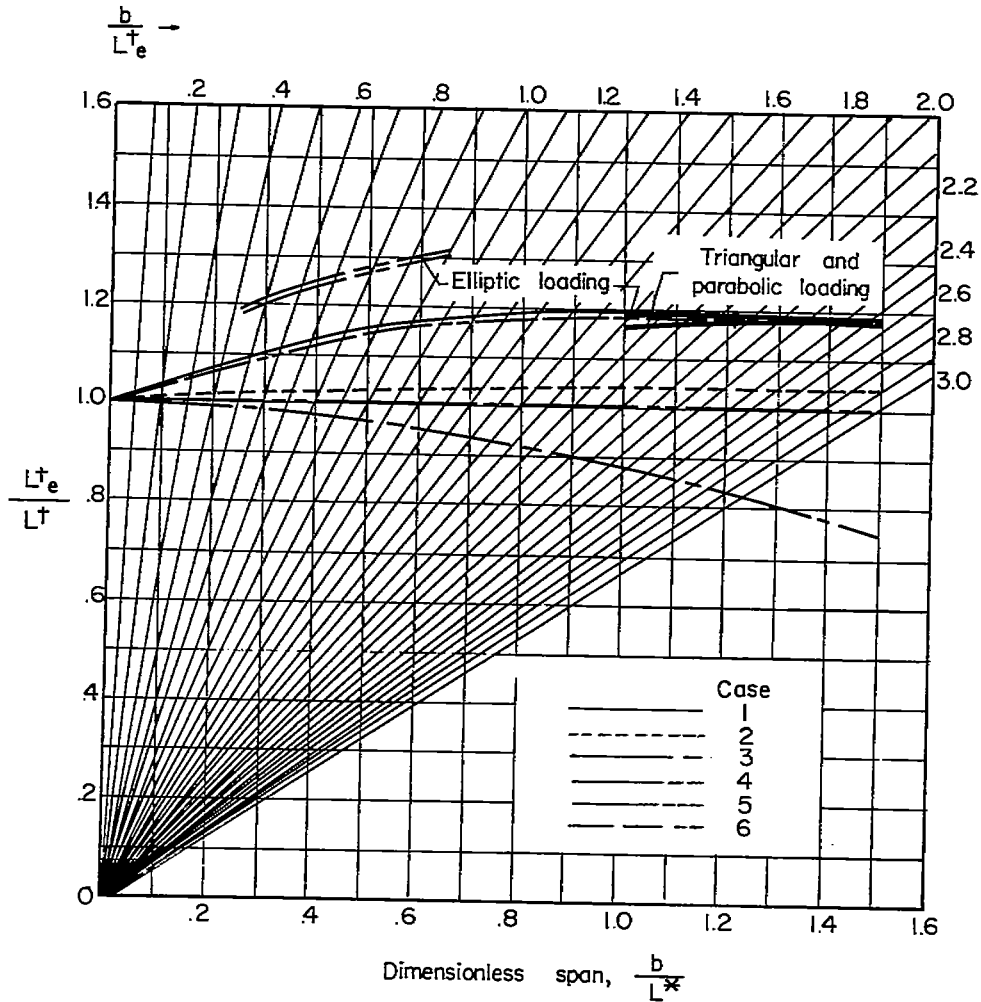


(d) Longitudinal spectra.

Figure 7.- Concluded.

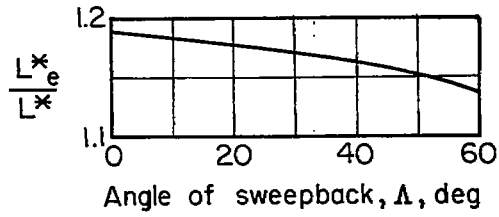


(a) Normal scales for swept wings with rectangular loading;
 $\frac{b}{L^*} \cos \Lambda = 0.5$.

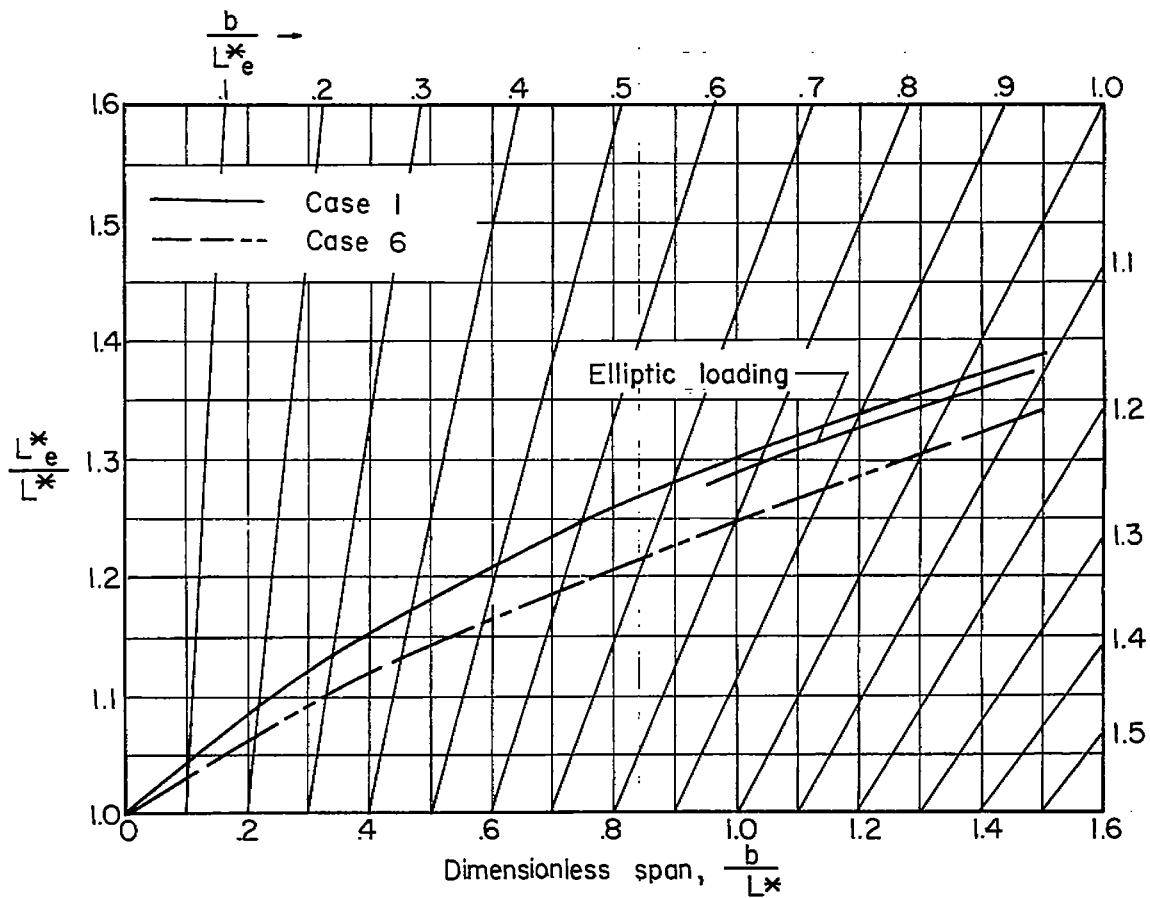


(b) Normal scales for unswept wings.

Figure 8.- Effective scales of turbulence.



(c) Longitudinal spectra for swept wings with rectangular loading;
 $\frac{b}{L^*} \cos \Delta = 0.5$.



(d) Longitudinal spectra for unswept wings.

Figure 8.- Concluded.